Potent Farnesyltransferase Inhibitors with 1,4-Diazepane Scaffolds as Novel Destabilizing Microtubule Agents in Hormone-Resistant Prostate Cancer

Nicolas Wlodarczyk,[†] Delphine Le Broc-Ryckewaert,[‡] Pauline Gilleron,[†] Amélie Lemoine,[†] Amaury Farce,[†] Philippe Chavatte,[†] Joëlle Dubois,[§] Nicole Pommery,[‡] Jean-Pierre Hénichart,[†] Christophe Furman,[‡] and Régis Millet*,[†]

[†]Institut de Chimie Pharmaceutique Albert Lespagnol, Université Lille-Nord de France, EA4481, IFR114, 3 Rue du Pr Laguesse, B.P. 83, F-59006 Lille, France

[‡]Faculté des Sciences Pharmaceutiques et Biologiques de Lille, Université Lille-Nord de France, EA4483, IFR114, 3 Rue du Pr Laguesse, B.P. 83, F-59006 Lille, France

[§]Institut de Chimie des Substances Naturelles, UPR2301 CNRS, Centre de Recherche de Gif, Avenue de la Terrasse, F-91198 Gif-sur-Yvette Cedex, France

S *Supporting Information*

ABSTRACT: A new class of potent farnesyltransferase inhibitors based on a 1,4-diazepane scaffold was synthesized with protein farnesyltransferase inhibition potencies in the low nanomolar range. The compounds block the growth on two hormone-resistant tumor prostatic cell lines (DU145 and PC3). The advanced cellular evaluation of the more potent farnesyltransferase inhibitors was explored and revealed a disorganization of tubulin in PC3 cells.
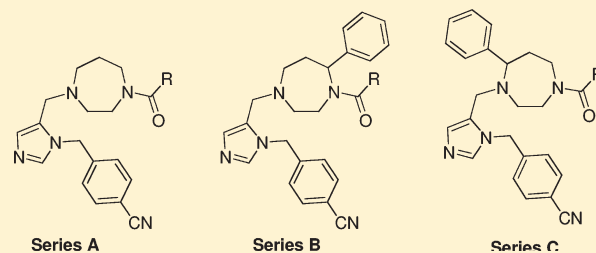
INTRODUCTION

The maturation of many proteins requires one or more post-translational modifications. Around 60 proteins are activated by a series of post-translational modifications: prenylation, proteolysis, and carboxymethylation.[1] The prenylation reaction is catalyzed by a zinc metalloenzyme: the farnesyltransferase (FTase) or geranylgeranyltransferase-I (GGTase-I).[2] This reaction results in the addition of a farnesyl (C15) or a geranylgeranyl (C20) moiety to the cysteine residue located at the C-terminal tetrapeptidic sequence called "CA$_1$A$_2$X box" (A$_1$A$_2$, aliphatic amino acids; X, methionine or serine for farnesyltransferase, leucine, or isoleucine for geranylgeranyltransferase I). The farnesylation provides sufficient hydrophobicity for the adequate cellular localization of proteins overactivated in some pathologies like cancer (Ras, Rheb, RhoB, CENP-E, -F). This overactivation can be induced either directly by mutation of the farnesylated protein or by mutation of an activator or an inactivator of farnesylated proteins. Therefore, the development of FTase inhibitors (FTis) represents a promising strategy in cancer therapy.[3]

FTis have demonstrated efficiency in the treatment of 70% of cancers cell lines in vitro.[4] To date, many compounds have been developed for clinical trials for the treatment of solid tumors and hematological malignancies. The three most studied are the R115777 (or tipifarnib), the SCH66336 (or lonafarnib), and

the BMS-214662 (Figure 1). Although efficient with low systemic toxicity in preclinical and animal models, no significant benefit has been observed for FDA approbation. However, synergistic or additive effects of combination of various FTis with some cytotoxic antineoplastic drugs (e.g., taxane, cisplatine) offer new perspectives for cancer treatment.[5−9] The exact biological mechanism by which FTis exert their antitumor activity remains controversial. Nevertheless, the discoveries of several farnesylated proteins with potent antitumor activity suggest that the mechanism results in the combination of effects of numerous proteins. For example, the centromere-associated proteins CENP-E constitute one pertinent target of FTis, since the elucidation of a functional association of CENP-E with microtubules requires farnesylation.[10]

Prostate cancer is the most frequently diagnosed malignancy in men in Europe and the United States.[11] Antiandrogenic treatments are often effective in the treatment of hormone-dependent prostate cancer. However, resistance against treatment often occurs as tumors acquire a hormone-refractory phenotype that does not respond to chemotherapy. This recurrent problem highlights the necessity to develop novel drugs for

the treatment of hormone-refractory prostate cancer. We therefore decided to focus the study of our FTis on whole cell assays using hormone-resistant prostate cancer cell lines derived from brain metastasis (DU145) and bone metastasis (PC3).

One of the possible approaches in the development of FTis is the design of peptidomimetics of the "CA$_1$A$_2$X box". Cocrystallization of FTase with numerous FTis or substrate has enabled the complete elucidation of FTase mechanism of action.[12−15] Thereafter, the design of FTis evolved from thiol-containing peptidomimetics[16] to non-thiol, non-peptidic molecules.[17−19] On the basis of these data and molecular modeling studies, we designed a pharmacophoric model based on a spacer that positioned correctly in the enzyme's active site a zinc chelator and a hydrophobic fragment. Molecular docking provided interesting features[17] in terms of key interactions between the p-cyanobenzylimidazole part with zinc and interaction between a hydrophobic part with a subsite called the "A$_2$ binding site". As part of our continuing effort to identify novel FTis, this information
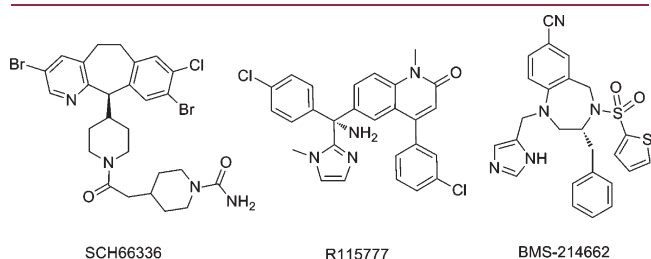
was used to design the novel, potent FTis structures shown in Figure 2. The p-cyanobenzylimidiazole zinc chelator was retained in this study, since ALIFT126 has exhibited low in vivo toxicity in our previous work.[19] The 1,4-diazepane scaffold confers the steric constraint with minimal peptidic features and higher metabolic stability to obtain the correct fit with the zinc and the "A$_2$ binding site".

The pharmacomodulations take place around the hydrophobic fragment. For the exploration of the structure−activity relationships (SARs), 19 different hydrophobic substituents (series A) were introduced on the 1,4-diazepane scaffold and SAR studies were completed by the synthesis of two further series of compounds (series B and C) bearing an additional phenyl group on the 1,4-diazepane scaffold. In light of these considerations, our efforts to identify new FTis have revealed three novel series of 1,4-diazepane and 5-phenyl-1,4-diazepane derivatives. Cellular activity against prostatic cell lines (DU145 and PC3) was determined as well as their effects on tubulin organization.

■ CHEMISTRY

The syntheses of diazepane derivatives are outlined in Schemes 1 and 2; structures of target amides (3−21, 28−33, and 46−51) are summarized in Tables 1, 2, and 3. The p-cyanobenzylimidazole moiety was introduced into target molecules according to a standard procedure of N-alkylation with the 5-chloromethyl-1-(4-cyanobenzyl)imidazole initially prepared.[20]

Compounds 3−21 were prepared in three steps from commercially available Boc-homopiperazine (series A, Scheme 1). Briefly, N-alkylation of Boc-homopiperazine with chloromethyl
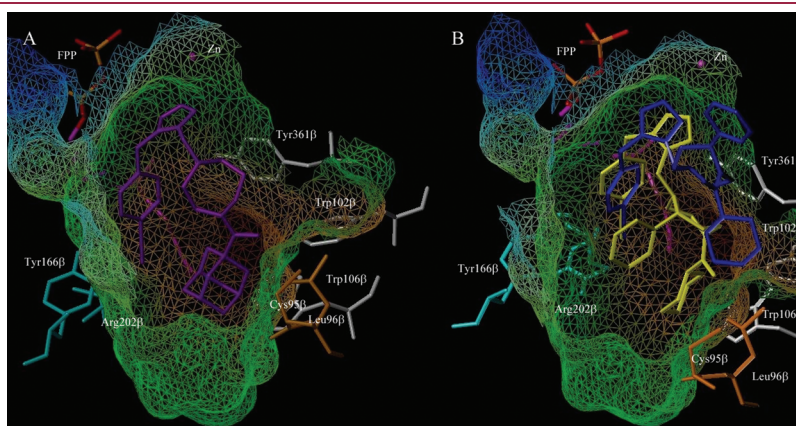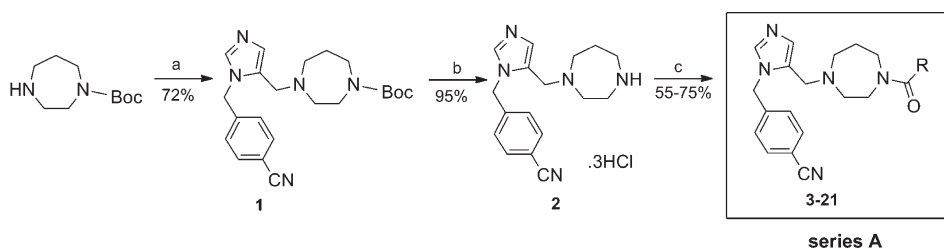

Figure 1. FTis developed to clinical trials.

Figure 2. (A) Docking of compound **20** (IC$_{50}$ = 5 nM) in the active site of the FTase. (B) Superimposition of compounds **32** (blue) and **50** (yellow) docked in the FTase binding site.

Scheme 1. Syntheses of Series A[a]

[a] Reagents and conditions: (a) 5-chloromethyl-1-(4-cyanobenzyl)imidazole, DIEA, ACN, 80 °C, 4 h; (b) HCl/^{i}PrOH, rt, 4 h; (c) R-COOH, PyBroP, PS-HOBt (HL), DIEA, DMF, rt, 20 h.

Scheme 2. Syntheses of Series B and C[a]
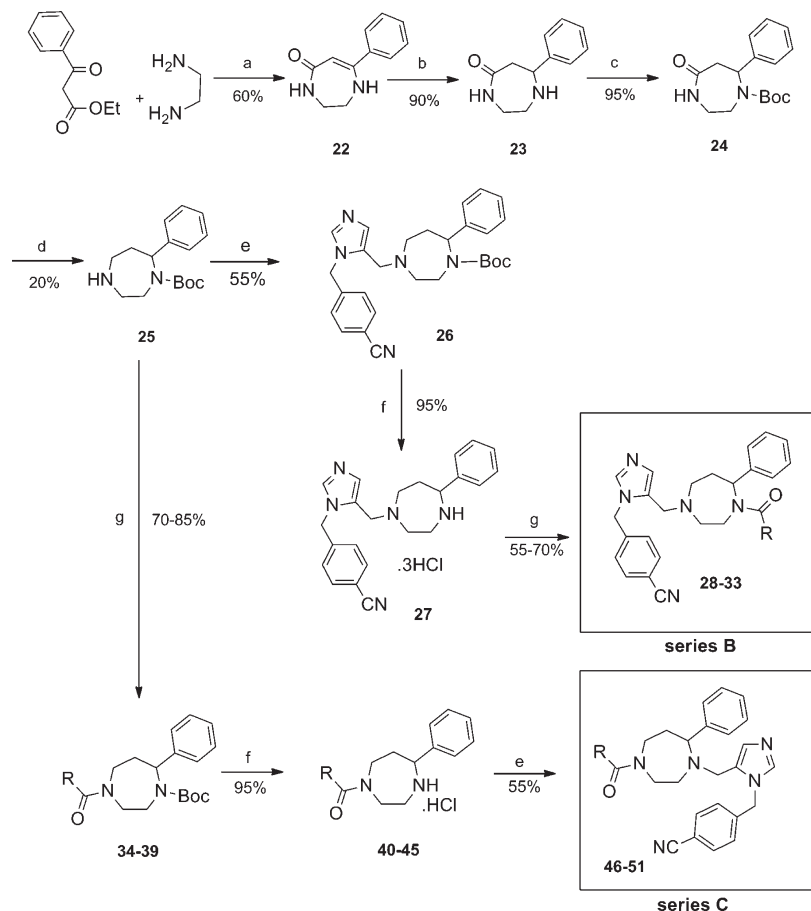
[a] Reagents and conditions: (a) xylene, reflux, 8 h; (b) H$_2$, 50 bar, 10% Pd/C, MeOH, 60 °C, 24 h; (c) (Boc)$_2$O, DIEA, dioxane/water (4:1), rt, 48 h; (d) LiAlH$_4$, THF, rt, 24 h; (e) 5-chloromethyl-1-(4-cyanobenzyl)imidazole, DIEA, ACN, 80 °C, 4 h; (f) ^{i}PrOH/HCl (5−6 N), rt, 2 h; (g) R-COOH, EDCI, DMAP, pyridine, DMF, rt, 18 h.

p-cyanobenzylimidazole gave compound **1**. After deprotection, the amine **2** was next coupled with a set of different carboxylic acids. Chemical diversity around the 1,4-diazepane scaffold was easily obtained by a solid-phase procedure using previously reported polystyrene-supported HOBt as coupling agent.[21] The reaction was performed on a Quest 205 synthesizer according to the general reaction pathway generating compounds **3−21**. This was a two-step procedure consisting of (i) formation of the polymer bound activated ester of the carboxylic acid using PyBrop and (ii) release of the target amide in solution by addition of the amine. Optimization of both steps was performed to obtain a solution of amide without byproducts. Optimum conditions for the activation step were found to be two periods of 2 h in DMF. The coupling step was achieved in 20 h with 0.6 equiv of the amine **2** in DMF.[22] The target compounds **3−21** were purified by preparative TLC.

Synthesis of 5-phenyl-1,4-diazepane derivatives (Scheme 2) was performed by the use of two different synthetic routes (series B and C) that both included the formation of the 4-Boc-5-phenyl-1,4-diazepane scaffold **25** previously described by our team.[23] Condensation of ethyl benzoylacetate with ethanediamine was carried out in xylene to yield enaminone **22** by azeotropic distillation. Reduction of the olefin by catalytic hydrogenation (H$_2$, 50 bar) gave 2-phenyl-1,4-diazepan-5-one
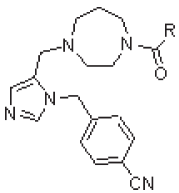
23. After carbamate protection of the secondary amine, the 1,4-diazepane scaffold **25** was obtained by lactam reduction with LiAlH$_4$.
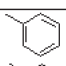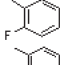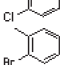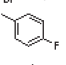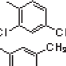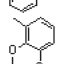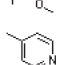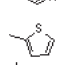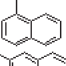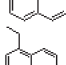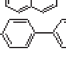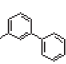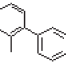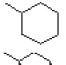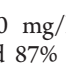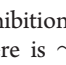
The target compounds **28−33** (series B) and **46−51** (series C) were finally obtained by classical methodology including alkylation of amines with chloromethylimidazole, cleavage of the Boc group, and acylation under peptide coupling conditions (EDCI/DMAP).

■ PHARMACOLOGICAL EVALUATION

All of the synthesized compounds were tested in a preliminary enzymatic assay and in a cytotoxicity assay on hormone-resistant prostate cancer DU145 and PC3 cell lines. The FTase assays were determined by measurement of the inhibition of human recombinant FTase which catalyzed the transfer of the FPP moiety to a fluorescent dansyl-GCVLS.[24] This fluorescent assay is easier and more rapid than conventional methods using radioactive substrates such as [^{3}H]FPP. Commercially available L-744,832 ((2S)-2-[[(2S)-2-[(2S,3S)-2-[(2R)-2-amino-3-mercaptopropyl]amino]-3-methylpentyl]oxy]-1-oxo-3-phenylpropyl]-amino]-4-(methylsulfonyl)-butanoic acid 1-methylethyl ester) was used as a reference compound.[25] L-744,832 has been reported to exhibit good pharmacological activity in hormone-resistant prostate cancer cell lines. Moreover, an in vivo study

Table 1. Structures and Biological Data of Compounds in Series A

Compounds	R	IC$_{50}$		
		FTase (nM)[a]	DU145 (μM)[b]	PC3 (μM)[b]
3		8	24% at 100 μM	22% at 100 μM
4		140	7% at 100 μM	2% at 100 μM
5		25	100	70
6		64	17% at 100 μM	15% at 100 μM
7		69	27% at 100 μM	40% at 100 μM
8		41	45	26
9		15	34% at 100 μM	0% at 100 μM
10		43	44% at 100 μM	80
11		142	6% at 100 μM	12% at 100 μM
12		42	3% at 100 μM	4% at 100 μM
13		39	44	65
14		35	52	47
15		13	93	40% at 100 μM
16		153	47	50
17		43	42	44
18		26	43	39
19		24	23% at 100 μM	20% at 100 μM
20		5	44	21
21		205	18% at 100 μM	13% at 100 μM
L-744,832		27	78	75

[a] Values are the mean of three determinations (standard deviation lower than 10%). [b] Cell proliferation was measured from at least three independent determinations (standard deviation lower than 10%).
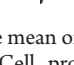
with L-744,832 on xenograft mice at 30 mg/kg showed a decrease of 85% of tumor on DU145 and 87% on PC3.[27] In our study, the IC$_{50}$ values for the growth inhibitions were 75 μM (PC3) and 78 μM (DU145). Indeed, there is ~300-fold difference of cytotoxicity between the IC$_{50}$ (PC3) evaluated in our cell culture conditions and that referenced in the literature (225 nM versus 75 μM, respectively).[26] No data were referenced for IC$_{50}$ on DU145 cell lines.

We started our investigations by evaluating the influence on enzymatic and cellular activity of the hydrophobic moiety at the 4-N-position of the 1,4-diazepane spacer (series A). The results are summarized in Table 1. All compounds inhibited FTase activity in the nanomolar range. These results allowed characterization of a first FTase inhibitory fragment based on the 1,4-

diazepane linked to 4-cyanobenzylimidazole. These observations suggested that the diazepane core constitutes a convenient linker. Compound 3, with a benzoyl substituent, is one of the most potent compounds of the series A with an IC$_{50}$ of 8 nM. The influence of the electronic character was then studied. No correlation can be established between the FTase inhibition and the electronic character of the aroyl moiety. The modification of the electronic density of the aroyl either by electron-donating level like methyl (9, IC$_{50}$ = 15 nM) and methoxy (10, IC$_{50}$ = 43 nM) or by withdrawing groups like fluorine (4, IC$_{50}$ = 140 nM), chlorine (5, IC$_{50}$ = 25 nM), and bromine (6, IC$_{50}$ = 64 nM) led to a decrease of FTase inhibition. Moreover, the displacement of fluorine from ortho (4) to para (7, IC$_{50}$ = 69 nM) enhances the activity and the introduction of a second

Table 2. Structures and Biological Data of Compounds in Series B

Compounds	R	IC$_{50}$		
		FTase (nM)[a]	DU145 (µM)[b]	PC3 (µM)[b]
L-744,832		27	78	75
28		79	75	80
29		382	31% at 100 µM	76
30		57	47	50
31		60	54	50
32		503	8% at 100 µM	5% at 100 µM
33		17	42	41

[a] Values are the mean of three determinations (standard deviation lower than 10%). [b] Cell proliferation was measured from at least three independent determinations (standard deviation lower than 10%).

Table 3. Structures and Biological Data of Compounds in Series C

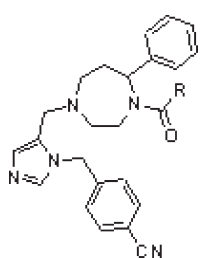| Compounds	R	IC$_{50}$		
		FTase (nM)[a]	DU145 (µM)[b]	PC3 (µM)[b]
L-744,832		27	78	75
46		9	73	33
47		21	44	38
48		17	35	50
49		18	48	77
50		7	29	18
51		6	32	32

[a] Values are the mean of three determinations (standard deviation lower than 10%). [b] Cell proliferation was measured from at least three independent determinations (standard deviation lower than 10%).
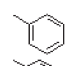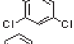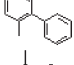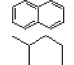
chlorine in compound **5** reduces affinity (**8**, IC$_{50}$ = 41 nM). From this observation, it seems that only the steric character of these groups modifies the activity rather than their electronic effect on the benzoyl.

Next, we investigated the modification of the phenyl group in **3** by bioisosters such as pyridinyl, thienyl, naphthyl, or biphenyl groups. Results confirmed that this modification affects affinity toward FTase. For example, the pyridinyl derivative **11** (IC$_{50}$= 142 nM) and thienyl derivative **12** (IC$_{50}$= 42 nM) displayed lower inhibitory potencies than **3**. A similar result was obtained for naphthyl derivatives **13** (α, IC$_{50}$ = 39 nM) and **14** (β, IC$_{50}$ = 35 nM). However, when the naphthyl moiety was positioned further away from the diazepane core (by a methylene) leading to compound **15** (IC$_{50}$ = 13 nM), inhibi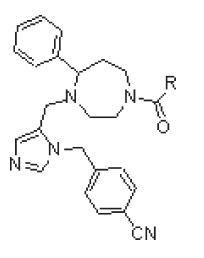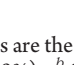tion of FTase was of the same magnitude as **3**. We also synthesized three biphenyl derivatives: FTase inhibitory activity of compounds **16** (IC$_{50}$ = 153 nM), **17** (IC$_{50}$ = 43 nM), and **18** (IC$_{50}$ = 26 nM) suggests that the hydrophobic cavity could be wide and shallow.

Different results were observed when the diazepane core was substituted by an aliphatic substituent. The isobutyl group (**21**, IC$_{50}$ = 205 nM) decreased markedly the interaction with the active site, whereas the adamantyl group (**20**, IC$_{50}$ = 5 nM) induced a slight increase in affinity and afforded the best FTase inhibitory potency of the series A. As a net result, the aromatic character of the terminal group does not appear to be critical for good affinity, while the steric parameter of this group is clearly of great importance. Any substitution on a benzoyl group tends to decrease the affinity in direct relation to the bulk introduced. On the other hand, a shorter moiety, such as the isobutyl of compound **21**, does not lead to a good affinity, presumably because it lacks a sufficient contact with the FTase pocket.

Only eight compounds (**5**, **8**, **13**, **14**, **16**, **17**, **18**, and **20**) among the 19 prepared exhibited cellular activity. Thus, some powerful inhibitors of FTase, like compound **3** with a phenyl

group, have no antiproliferative activity on DU145 or PC3 cell lines. These eight compounds all exhibited a better cellular efficiency than L-744,832. The best cellular activities were observed with the 2,4-dichlorophenyl (**8**) (IC$_{50}$(DU145) = 45 µM, IC$_{50}$(PC3) = 26 µM) and the adamantyl (**20**) (IC$_{50}$(DU145) = 44 µM, IC$_{50}$(PC3) = 21 µM). No correlation in the series A was observed between the FTase inhibition and the cell growth inhibition on the two cell lines. Among many factors influencing the cell-based assay activity, the cell membrane penetration of FTis is certainly important. The low cellular activity of many of the compounds studied here could be explained by a lack of lipophilicity. The addition of a chlorine atom (**8**) to compound **5** decreased the FTase activity but increased the whole cell assay. This observation could only be explained by the improvement of cell penetration facilitated by increased lipophilicity (**5**, CLogP = 2.73; **8**, CLogP = 3.47).[28] It is worth pointing out that all compounds exhibited antiproliferative activity in excess of their intrinsic activity against FTase. Though rare, this phenomenon has been reported in other publications.[29,30]

Next, we decided to retain the diazepane scaffold and to develop two series (B and C) of potent FTase inhibitors bearing a phenyl group on the scaffold in order to improve their lipophilic character and to procure an additional interaction with the enzyme. Two alkyl groups (cyclohexyl and adamantyl) and four aryl groups (phenyl, 2,4-dichlorophenyl, naphthyl, and o-biphenyl) were introduced. The enzymatic studies revealed different results between series B and C derivatives and showed that the position of the phenyl group around the spacer was important for optimal interaction with the active site. The FTase activity of series B derivatives (IC$_{50}$ = 17−503 nM) was less than those of series C (IC$_{50}$ = 6−27 nM). In addition, when looking at compounds **28**−**33**, we found that series B compounds had a

slightly lower affinity compared with their nonsubstituted analogues in series A (**3**, **8**, **13**, **18**, **19**, and **20**).

As expected, the cellular activity of compounds in both series B and C generally followed the FTase assay results. The majority of these FTis exhibited better cell growth inhibition than the reference inhibitor L-744,832. The cyclohexyl derivative **50** displayed the best cellular activities (IC_{50}(DU145) = 29 μM and IC_{50}(PC3) = 18 μM). The addition of a phenyl group at the C-5-position of diazepane improved only slightly the FTase inhibition (**50**, IC_{50} = 7 nM) but significantly enhanced the cell growth inhibition on both cell lines. This observation supports the hypothesis that the low lipophilicity of many compounds in series A limited their cellular activity. The phenyl bearing at the C-5-position of the diazepane scaffold increases the lipophilicity which is necessary for membrane penetration and subsequent inhibition of cell proliferation.

PHARMACOKINETIC STUDIES IN VITRO

Pharmacokinetic data for compounds **20**, **50**, and **51** were collected on Caco2 cells to evaluate their absorption potency in an in vitro model and in human liver microsomes to assess their metabolic stability.[31] Compounds **20** and **50** revealed an apparent permeability coefficient (P_{app}) value of 28.8 × 10^{-6} and 25.1 × 10^{-6} cm/s, respectively, and are therefore considered highly permeable. Evaluation of compound **51** revealed a P_{app} value of 3.6 × 10^{-6} cm/s, which is indicative of a medium permeable molecule. In this assay, propranolol was used as a highly permeable reference (P_{app} = 41.1 × 10^{-6} cm/s), labetalol as a medium permeable reference (P_{app} = 7.3 × 10^{-6} cm/s), and ranitidine as a low permeable reference (P_{app} = 0.7 × 10^{-6} cm/s), according to the FDA guidance.[32] Furthermore, metabolic stability of these compounds were evaluate in human liver microsomes and showed a poor stability as the percentage of remaining parent drug at the end of the assay were 1%, 2%, and 3% for compounds **20**, **50**, and **51**, respectively. For metabolic stability assays, propanolol, terfenadine, and verapamil were used as references (percentage of remaining parent drug at the end of the assay: 60, 6 and 9% respectively).

MOLECULAR MODELING

Docking simulations,[33] using GOLD software, were carried out in order to clarify the binding mode of FTis at the active site of FTase (Figure 2). Thirty-one solutions were generated for each compound, then ranked according to an in-house scoring function. The consistency of the best ranked solution was assessed by manually inspecting the conformations. The pharmacological results were concordant with molecular modeling which provides a reasonable explanation for their inhibitory activity.

Compound **19** is too small to have a well-defined binding mode. Its small size enables it to adopt a large number of conformations, none of them being predominant among the best ranked solutions. Only one solution displayed the same U shape, as the ligand used crystallized previously with the enzyme.[34] For compound **50**, the benzyl group on the diazepane is oriented toward the opening of the binding site in a conformation that is clearly poorer because it is unable to form any interaction. Its terminal cyclohexyl occupies the depth of the pocket, surrounded by Trp 102β and 106β. Compound **32** displayed evenly distributed conformations in the expected U shape and the other conformations, directing it toward the entry
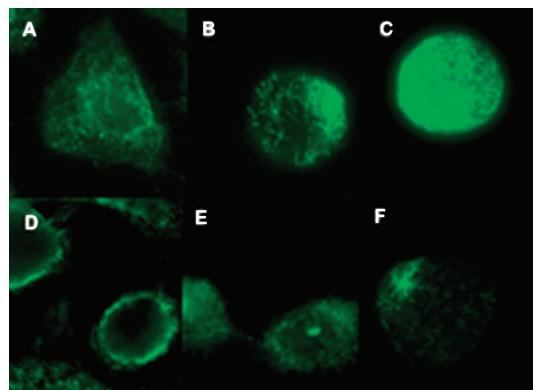
Figure 3. Immunofluorescent visualization of the tubulin network in control (A) and in treated (B−F) PC3 cells. Cells were treated for 24 h both in the absence and in the presence of 21, 18, and 32 μM compounds **20**, **50**, and **51**, respectively (D, E, F), and microtubules were visualized by immunofluorescence labeling using an antibody against α-tubulin. Treatment with CA-4 (3 nM (B)) and L-744,832 (75 μM (C)) were included as positive controls.

of the pocket. From an atomic point of view, the best conformations of these three compounds were very similar to each other (**19**, **32**, and **50**), with the positioning of the cyclohexyl group nearly superimposable. It is also of interest to note that the adamantyl of compounds **20** and **33** also occupies the same position in the binding site, implying that a bulky aliphatic group is more favorably bound in the portion of the pocket, delineated by Trp102β, Trp106β, and Tyr361β (the "A_2 binding site"). At the other end of the compounds, the imidazole nitrogen coordinates with the zinc of the enzyme while the cyano moiety is engaged in a hydrogen bond with Arg202. The most numerous conformations of compounds **32** and **50** offer an explanation for the better potency of series C. Although the best-ranked conformation of **32** binds in a conformation very close to that of compound **50**, it is also very uncommon in the pool of solutions. The most numerous binding mode of **32** is shown in Figure 2. It is characterized by the placement of the phenyl and the terminal cyclohexyl at the very gate of the pocket, where they do not contribute to the affinity of the compound. As there is no high energy interaction present to anchor the inhibitor to the enzyme, such a binding mode can only be described as potentially unstable and weak.

IMPACT OF FTIS ON TUBULIN ORGANIZATION

Some recent studies have revealed that FTis such as lonafarnib (or SCH66336) were involved in the destabilization of the tubulin network.[35] We wanted to know, in this part of the study, if the more potent FTis defined earlier (compounds **20**, **50**, and **51**) were able to affect microtubule organization in PC3 cells. Thus, PC3 cells were treated with the three compounds of interest for 24 h. After fixing and permeabilization, microtubules were visualized by indirect immunofluorescence microscopy using an antibody against α-tubulin. Cells treated with DMSO (control cells) exhibited a well-organized microtubule network throughout the cells (Figure 3A). In contrast, cells treated with CA-4 (positive control, Figure 3B), known to bind tubulin at the colchicine site and to destabilize microtubules by the inhibition of assembly of tubulin molecules,[36] showed a disruption of the tubulin network and the appearance of a bundle at a pole of the cell compared with DMSO treated cells. Treatment with 75 μM
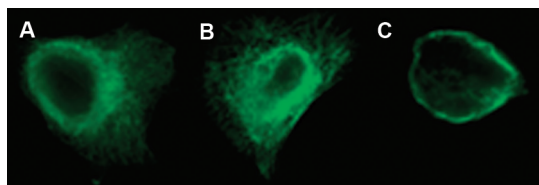
Figure 4. Immunofluorescent visualization of the tubulin network in CENP-E knockdown PC3 cells (C) and control siRNA-transfected cells (B) compared to DMSO treated cells (A).

of L-744,832 (FTis positive control, Figure 3C) led to the formation of similar microtubule bundles observed in the CA-4 treated cells. Cells treated with compounds **20**, **50**, and **51** at concentrations equal to their IC$_{50}$ values displayed a completely disorganized tubulin network restricted to the periphery of PC3 cells (Figure 3C, Figure 3E, and Figure 3F, respectively). Moreover, with these compounds, the microtubule mass appeared to be decreased compared with control cells, especially for compounds **50** and **51**.

Aberrant spindle formation following treatment with FTis was related, in previous work,[37,38] to the disruption of farnesylated mitotic proteins' functionality, CENP-E and CENP-F, known to be strongly involved in kinetochore-microtubule interactions. To assess the role of CENP-E in PC3 cells as one of the targets associated with the tubulin network destabilization following FTis treatment, we suppressed CENP-E expression by using CENP-E siRNA. This approach led to a 90% decrease in CENP-E expression in our cells (data not shown). Compared to controls or to GAPDH siRNA transfected cells, CENP-E siRNA transfected cells exhibited a completely disorganized tubulin network (Figure 4) similar to PC3 cells treated with the compound **20**.

■ CONCLUSION

This study has shown that the 1,4-diazepane scaffold constitutes an effective platform for the development of novel inhibitors. Thirty-one compounds were synthesized and most of them exhibited nanomolar affinity for an isolated FTase enzyme as well as cellular activity on two hormone refractory prostate cancer cell lines (PC3 and DU145).

Examination of the SAR of these compounds revealed interesting information about their interactions with the active site of the FTase. In series A (with no phenyl on the spacer), modulation of 19 substituents enabled us to demonstrate that this group FTis fits principally by hydrophobic interactions with a pocket delineated by Trp102β, Trp106β, and Tyr361β. Moreover, the correct addition of a phenyl group on the diazepane scaffold (series C vs series B) proved to be necessary to increase the cellular activity without loss of FTase inhibition and to increase the lipophilicity of the compounds.

The permeation ability of compounds **20**, **50**, and **51** through biological membranes was assessed on Caco2 cells to evaluate their potential for gastrointestinal absorption. **20** and **50** were predicted to be "highly permeable" and therefore conveniently enter blood circulation. **51** was predicted to have "medium permeability". However, these compounds exhibited a poor metabolic stability, suggesting that a peroral administration is to be avoided because of the first-pass effect. These preliminary in vitro results are the first step for a fully in vivo evaluation.

In this study, we have shown for the first time in the prostatic hormone-independent PC3 cell line a disruption of the tubulin network by FTis. These results are in agreement with previous observed data. Except for the classical targets of FTis like Ras and RhoB, involved in the antiproliferative and cytotoxic activities of these compounds, the function of CENP-E, which mediates cell cycle progression by chromosome capture and alignment and is a known farnesylated mitotic protein, was also investigated in this study. Depletion of CENP-E in our cells, by transfecting the appropriate siRNA, led to a disruption of the tubulin network similar to that observed with treatment of PC3 by the compound **20**. We therefore hypothesize that in PC3 cells, inhibition of CENP-E farnesylation by compound **20** led to a loss of CENP-E activity and tubulin network disruption. Since another farnesylated mitotic protein, CENP-F, is known to be required in cell cycle progression, it would be interesting to test the ability of our compounds to block the cell cycle in G2-M. Furthermore, studies concerning the combined use of our potent FTis with microtubule interfering agents are in progress, as this association presents an effective antiproliferative and antimitotic synergy.

■ EXPERIMENTAL SECTION

Chemistry. General Remarks. All commercial reagents and solvents were used without further purification. Analytical thin-layer chromatography was performed on precoated Kieselgel 60F$_{254}$ plates (Macherey Nagel); the spots were visualized by UV (254 and 366 nm) and/or with iodine. Silica gel grade 60 (230−400 mesh) purchased from Macherey Nagel was used to carry out chromatographic separation. Preparative thin layer chromatography (TLC) was performed using silica gel from Macherey Nagel, the compounds being extracted from the silica using CH$_2$Cl$_2$/MeOH (8:2 v/v). All melting points were determined with a Büchi 535 capillary apparatus and remained uncorrected. ^{1}H NMR spectra were obtained using a Bruker 300 MHz spectrometer. Chemical shifts (δ) were expressed in ppm relative to tetramethylsilane used as an internal standard. J values are in hertz, and the splitting patterns were designated as follows: s singlet, d doublet, t triplet, m multiplet. HPLC−MS analyses were accomplished using a HPLC instrument combined with a Surveyor MSQ (Thermo Electron) equipped with an APCI source (ODS-30 column, mobile phase of water/acetonitrile/formic acid, gradient mode). Elemental analyses for all compounds were performed by the "Service Central d'Analyses" at the CNRS, Vernaison, France. All tested target compounds possessed a purity of ≥95% as verified by HPLC−MS or elemental analysis (C, H, N).

***N*-1-*tert*-Butoxycarbonyl-*N*-4-[1-(4-cyanobenzyl)-1*H*-5-imidazolyl]methyl-1,4-diazepane (1).** Boc-homopiperazine (3.09 mL, 15.7 mmol) was added to a solution of 2-chloromethyl-1(4-cyanobenzyl)-imidazole (3.5 g, 13.1 mmol) and DIEA (6.82 mL, 39.2 mmol) in 40 mL of ACN. The reaction mixture was stirred for 4 h at 80 °C and then concentrated under vacuum. The residue was dissolved in EtOAc and washed with water and brine. The organic layer was dried over MgSO$_4$, filtered, and evaporated. The residue was purified by column chromatography on silica gel (CH$_2$Cl$_2$/MeOH 96:4) to give a white powder (3.73 g, 72% yield). R_f = 0.65 (CH$_2$Cl$_2$/MeOH 9:1). Mp: 131−133 °C. IR (neat): ν 2229 (CN), 1683 (CO). ^{1}H NMR (DMSO-d_6): δ 1.45 (s, 9 H), 2.45−2.60 (m, 4 H), 3.31 (s, 2 H), 3.31−3.46 (m, 6 H), 5.38 (s, 2 H), 6.97 (s, 1 H), 7.16 (d, J = 7.9 Hz, 2 H), 7.56 (s, 1 H), 7.63 (d, J = 7.9 Hz, 2 H). MS (APCI$^+$) m/z = 396 (M + H$^+$).

4-[1-(4-Cyanobenzyl)-1*H*-5-imidazolyl]methyl-1,4-diazepane Hydrochloride (2). A solution of 5−6 N HCl in isopropanol was added to a solution of compound **1** (1 g, 2.53 mmol) in MeOH (2 mL). After the mixture was stirred for 4 h at room temperature, the solvent was removed under vacuum. The solid was washed with diethyl ether and recrystallized in absolute EtOH to give a white powder (0.97 g, 95% yield). R_f = 0.35 (CH$_2$Cl$_2$/MeOH 9:1). Mp: 152−154 °C. IR (neat): ν 2228 (CN). ^{1}H NMR (DMSO-d_6): δ 3.10−3.90 (m, 10 H),

4.43 (s, 2 H), 5.82 (s, 2 H), 7.57 (d, J = 7.9 Hz, 2 H), 7.92 (d, J = 7.9 Hz, 2 H), 8.11 (s, 1H), 9.31 (s, 1 H), 9.64 (bs, 1 H). MS (APCI$^+$) m/z = 296 (M + H$^+$).

General Procedure for Synthesis of 1-[1-(4-Cyanobenzyl)-1*H*-imidazol-5-yl]methyl-1,4-diazepanes (Compounds 3–21). An amount of 1.18 g of PS-HOBt (HL) resin was added to a 100 mL polypropylene Quest 205 reaction vessel and swelled in anhydrous DMF (10 mL) at room temperature. After 24 h, the solvent was filtered and a solution of carboxylic acid (2.32 mmol), DIEA (0.81 mL, 4.64 mmol), and PyBroP (1.08 g, 2.32 mmol) in anhydrous DMF (20 mL) was added. The mixture was stirred at room temperature for 2 h and filtered. The resin was washed successively with DMF (2 × 10 mL), DCM (2 × 10 mL), and DMF (2 × 10 mL). The same activation procedure was repeated a second time. Then a solution of amine **2** (500 mg, 1.24 mmol) and diisopropylethylamine (0.81 mL, 4.64 mmol) in DMF (20 mL) was added, and the reaction mixture was stirred for 20 h at room temperature. The supernatant was then separated from the resin, and the polymer beads were washed with DMF (2 × 10 mL), DCM (2 × 10 mL), and DMF (2 × 10 mL). The combined solutions were concentrated, and the residue was purified by preparative TLC on silica gel (DCM/MeOH 95:5). The product was then added to a solution of 5–6 N HCl in ^{i}PrOH and stirred for 1 h at room temperature. After addition of diethyl ether, the solid was filtered off, washed with diethyl ether, and recrystallized from EtOH/Et$_2$O to give a white powder.

*1-[1-(4-Cyanobenzyl)-1H-imidazol-5-yl]methyl-4-benzoyl-1,4-diazepane Hydrochloride (**3**).* 60% yield. R_f = 0.36 (CH$_2$Cl$_2$/MeOH 9:1). Mp: 168–171 °C. IR (neat): ν 2228 (CN), 1623 (CO). ^{1}H NMR (DMSO-d_6): δ 3.15–3.85 (m, 10 H), 4.51 (s, 2 H), 5.84 (s, 2 H), 7.32–7.50 (m, 5 H), 7.57 (d, J = 7.3 Hz, 2 H), 7.91 (d, J = 7.0 Hz, 2 H), 8.18 (s, 1 H), 9.29 (s, 1 H), 12.13 (bs, 1 H). MS (APCI$^+$) m/z = 400.2 (M + H$^+$). Anal. (C$_{24}$H$_{25}$N$_5$O·2HCl·2.5H$_2$O) C, H, N, Cl.

*1-[1-(4-Cyanobenzyl)-1H-imidazol-5-yl]methyl-4-(2-fluorobenzoyl)-1,4-diazepane Hydrochloride (**4**).* 56% yield. R_f = 0.63 (CH$_2$Cl$_2$/MeOH 9:1). Mp: 162–163 °C. IR (neat): ν 2228 (CN), 1623 (CO). ^{1}H NMR (DMSO-d_6): δ 3.15–3.85 (m, 10 H), 4.51 (s, 2 H), 5.84 (s, 2 H), 7.17–7.58 (m, 5 H), 7.83–7.95 (m, 3 H), 8.18 (s, 1 H), 9.12 (s, 1 H), 12.13 (bs, 1 H). MS (APCI$^+$) m/z = 418 (M + H$^+$). Anal. (C$_{24}$H$_{24}$FN$_5$O·2HCl·1.5H$_2$O) C, H, N, Cl.

*1-[1-(4-Cyanobenzyl)-1H-imidazol-5-yl]methyl-4-(2-chlorobenzoyl)-1,4-diazepane Hydrochloride (**5**).* 52% yield. R_f = 0.47 (CH$_2$Cl$_2$/MeOH 9:1). Mp: 139–141 °C. IR (neat): ν 2230 (CN), 1623 (CO). ^{1}H NMR (DMSO-d_6): δ 3.19–3.88 (m, 10 H), 4.50 (s, 2 H), 5.85 (s, 2 H), 7.48–7.71 (m, 6 H), 7.85 (s, 1 H), 7.89 (d, J = 7.2 Hz, 2 H), 9.26 (s, 1 H), 12.18 (bs, 1 H). MS (APCI$^+$) m/z = 433.9 (M + H$^+$). Anal. (C$_{24}$H$_{24}$ClN$_5$O·2HCl·2H$_2$O) C, H, N, Cl.

*1-[1-(4-Cyanobenzyl)-1H-imidazol-5-yl]methyl-4-(2-bromobenzoyl)-1,4-diazepane Hydrochloride (**6**).* 46% yield. R_f = 0.55 (CH$_2$Cl$_2$/MeOH 9:1). Mp: 178–180 °C. IR (neat): ν 2228 (CN), 1625 (CO). ^{1}H NMR (DMSO-d_6): δ 3.28–3.92 (m, 10 H), 4.50 (s, 2 H), 5.85 (s, 2 H), 7.44–7.62 (m, 6 H), 7.82 (s, 1 H), 7.90 (d, J = 7.2 Hz, 2 H), 9.25 (s, 1 H), 12.20 (bs, 1 H). MS (APCI$^+$) m/z = 478.1 (M + H$^+$). Anal. (C$_{24}$H$_{24}$BrN$_5$O·2HCl·2H$_2$O) C, H, N, Cl.

*1-[1-(4-Cyanobenzyl)-1H-imidazol-5-yl]methyl-4-(4-fluorobenzoyl)-1,4-diazepane Hydrochloride (**7**).* 43% yield. R_f = 0.45 (CH$_2$Cl$_2$/MeOH 9:1). Mp: 95–97 °C. IR (neat): ν 2230 (CN), 1638 (CO). ^{1}H NMR (DMSO-d_6): δ 3.30–3.90 (m, 10 H), 4.52 (s, 2 H), 5.82 (s, 2 H), 7.48–7.68 (m, 6 H), 7.75 (s, 1 H), 7.92 (d, J = 7.5 Hz, 2 H), 9.22 (s, 1 H), 12.22 (bs, 1 H). MS (APCI$^+$) m/z = 418.0 (M + H$^+$). Anal. (C$_{24}$H$_{24}$FN$_5$O·2HCl·1H$_2$O) C, H, N, Cl.

*1-[1-(4-Cyanobenzyl)-1H-imidazol-5-yl]methyl-4-(2,4-dichlorobenzoyl)-1,4-diazepane Hydrochloride (**8**).* 40% yield. R_f = 0.45 (CH$_2$Cl$_2$/MeOH 9:1). Mp: 192–193 °C. IR (neat): ν 2230 (CN), 1635 (CO). ^{1}H NMR (DMSO-d_6): δ 3.28–3.96 (m, 10 H), 4.38–4.51 (m, 2 H), 5.85 (s, 2 H), 7.48–7.68 (m, 5 H), 7.75 (s, 1 H), 7.90 (d, J = 7.2 Hz, 2 H),

9.26 (s, 1 H), 12.22 (bs, 1 H). MS (APCI$^+$) m/z = 468.0 (M + H$^+$). Anal. (C$_{24}$H$_{23}$Cl$_2$N$_5$O·2HCl·1.5H$_2$O) C, H, N, Cl.

*1-[1-(4-Cyanobenzyl)-1H-imidazol-5-yl]methyl-4-(3-toluyl)-1,4-diazepane Hydrochloride (**9**).* 61% yield. R_f = 0.65 (CH$_2$Cl$_2$/MeOH 9:1). Mp: 156–157 °C. IR (neat): ν 2228 (CN), 1623 (CO). ^{1}H NMR (DMSO-d_6): δ 2.34 (s, 3 H) ; 3.15–3.85 (m, 10 H), 4.51 (s, 2 H), 5.84 (s, 2 H), 7.17–7.39 (m, 4 H,), 7.41–7.57 (m, 2 H), 7.83–7.95 (m, 2 H), 8.18 (bs, 1 H), 9.12 (s, 1 H), 12.13 (bs, 1 H); MS (APCI$^+$) m/z = 414 (M + H$^+$); Anal. (C$_{25}$H$_{27}$N$_5$O·2HCl·1.5H$_2$O) C, H, N, Cl.

*1-[1-(4-Cyanobenzyl)-1H-imidazol-5-yl]methyl-4-(2,3-dimethoxybenzoyl)-1,4-diazepane Hydrochloride (**10**).* 60% yield. R_f = 0.44 (CH$_2$Cl$_2$/MeOH 9:1). Mp: 143–145 °C. IR (neat): ν 2230 (CN), 1623 (CO). ^{1}H NMR (DMSO-d_6): δ 2.98–3.69 (m, 10 H), 3.71 (s, 3 H), 3.83 (s, 3 H), 4.42 (s, 2 H), 5.80 (s, 2 H), 6.82–6.92 (m, 1 H), 7.06–7.15 (d, J = 8.0 Hz, 2 H), 7.49–7.61 (m, 2 H), 7.92 (d, J = 8.2 Hz, 2 H), 8.15 (s, 1 H), 9.18 (bs, 1 H), 12.12 (bs, 1 H). MS (APCI$^+$) m/z = 460.1 (M + H$^+$). Anal. (C$_{26}$H$_{29}$N$_5$O$_3$·2HCl·1.5H$_2$O) C, H, N, Cl.

*1-[1-(4-Cyanobenzyl)-1H-imidazol-5-yl]methyl-4-(4-pyridinoyl)-1,4-diazepane Hydrochloride (**11**).* 52% yield. R_f = 0.17 (CH$_2$Cl$_2$/MeOH 9:1). Mp: 210–212 °C. IR (neat): ν 2229 (CN), 1627 (CO). ^{1}H NMR (DMSO-d_6): δ 3.10–3.85 (m, 10 H), 4.48 (s, 2 H), 5.82 (s, 2 H), 7.28 (d, J = 8.0 Hz, 2 H), 7.55–7.78 (m, 4 H), 8.13 (s, 1 H), 8.92 (m, 2 H), 9.23 (s, 1 H), 12.32 (bs, 1 H). MS (APCI$^+$) m/z = 401.2 (M + H$^+$). Anal. (C$_{23}$H$_{24}$N$_6$O·3HCl·3H$_2$O) C, H, N, Cl.

*1-[1-(4-Cyanobenzyl)-1H-imidazol-5-yl]methyl-4-(3-thenoyl)-1,4-diazepane Hydrochloride (**12**).* 54% yield. R_f = 0.33 (CH$_2$Cl$_2$/MeOH 9:1). Mp: 214–216 °C. IR (neat): ν 2230 (CN), 1631 (CO). ^{1}H NMR (DMSO-d_6): δ 3.18–3.92 (m, 10 H), 4.48 (s, 2 H), 5.80 (s, 2 H), 7.02–7.10 (m, 1 H), 7.46 (s, 1 H), 7.52 (d, J = 8.0 Hz, 2 H), 7.76 (m, 1 H), 7.92 (d, J = 7.9 Hz, 2 H), 8.13 (s, 1 H), 9.22 (s, 1 H), 12.15 (bs, 1 H). MS (APCI$^+$) m/z = 406.2 (M + H$^+$). Anal. (C$_{22}$H$_{23}$N$_5$OS·2HCl·2H$_2$O) C, H, N, Cl.

*1-[1-(4-Cyanobenzyl)-1H-imidazol-5-yl]methyl-4-(1-naphtoyl)-1,4-diazepane Hydrochloride (**13**).* 68% yield. R_f = 0.42 (CH$_2$Cl$_2$/MeOH 9:1). Mp: 228–230 °C. IR (neat): ν 2228 (CN), 1641 (CO). ^{1}H NMR (DMSO-d_6): δ 3.15–3.95 (m, 10 H), 4.48 (s, 2 H), 5.82 (s, 2 H), 7.40–7.60 (m, 5 H), 7.85–8.05 (m, 6 H), 8.21 (s, 1 H), 9.27 (s, 1 H), 12.22 (bs, 1 H). MS (APCI$^+$) m/z = 450.1 (M + H$^+$). Anal. (C$_{28}$H$_{27}$N$_5$O·2HCl·3H$_2$O) C, H, N, Cl.

*1-[1-(4-Cyanobenzyl)-1H-imidazol-5-yl]methyl-4-(2-naphthoyl)-1,4-diazepane Hydrochloride (**14**).* 62% yield. R_f = 0.39 (CH$_2$Cl$_2$/MeOH 9:1). Mp: 224–226 °C. IR (neat): ν 2229 (CN), 1627 (CO). ^{1}H NMR (DMSO-d_6): δ 3.15–3.85 (m, 10 H), 4.48 (s, 2 H), 5.82 (s, 2 H), 7.50–7.65 (m, 5 H), 7.85–8.08 (m, 6 H), 8.13 (s, 1 H), 9.18 (s, 1 H), 12.13 (bs, 1 H). MS (APCI$^+$) m/z = 450.2 (M + H$^+$). Anal. (C$_{28}$H$_{27}$N$_5$O·2HCl·2H$_2$O) C, H, N, Cl.

*1-[1-(4-Cyanobenzyl)-1H-imidazol-5-yl]methyl-4-[2-(1-naphtyl)acetyl]-1,4-diazepane Hydrochloride (**15**).* 53% yield. R_f = 0.45 (CH$_2$Cl$_2$/MeOH 9:1). Mp: 216–218 °C. IR (neat): ν 2229 (CN), 1614 (CO). ^{1}H NMR (DMSO-d_6): δ 3.22–3.82 (m, 10 H), 3.88 (s, 2 H), 4.48 (s, 2 H), 5.82 (s, 2 H), 6.88 (m, 1 H), 7.50–7.65 (m, 4 H), 7.85–8.08 (m, 6 H), 8.13 (s, 1 H), 9.16 (s, 1 H), 12.18 (bs, 1 H). MS (APCI$^+$) m/z = 464.3 (M + H$^+$). Anal. (C$_{29}$H$_{29}$N$_5$O·2HCl·2H$_2$O) C, H, N, Cl.

*1-[1-(4-Cyanobenzyl)-1H-imidazol-5-yl]methyl-4-(4-phenylbenzoyl)-1,4-diazepane Hydrochloride (**16**).* 56% yield. R_f = 0.42 (CH$_2$Cl$_2$/MeOH 9:1). Mp: 231–233 °C. IR (neat): ν 2230 (CN), 1635 (CO). ^{1}H NMR (DMSO-d_6): δ 3.12–3.85 (m, 10 H), 4.48 (s, 2 H), 5.83 (s, 2 H), 7.38–7.62 (m, 7 H), 7.67–7.79 (m, 4 H), 7.92 (d, J = 7.9 Hz, 2 H), 8.15 (s, 1 H), 9.22 (s, 1 H), 12.17 (bs, 1 H). MS (APCI$^+$) m/z = 476.2 (M + H$^+$). Anal. (C$_{30}$H$_{29}$N$_5$O·2HCl·2H$_2$O) C, H, N, Cl.

*1-[1-(4-Cyanobenzyl)-1H-imidazol-5-yl]methyl-4-(3-phenylbenzoyl)-1,4-diazepane Hydrochloride (**17**).* 55% yield. R_f = 0.42 (CH$_2$Cl$_2$/MeOH 9:1). Mp: 247–248 °C. IR (neat): ν 2230 (CN), 1630 (CO). ^{1}H NMR (DMSO-d_6): δ 3.15–3.85 (m, 10H), 4.44 (s, 2 H), 5.83 (s, 2 H),

7.34−7.60 (m, 7 H), 7.67−7.79 (m, 4 H), 7.92 (d, J = 7.9 Hz, 2 H), 8.15 (s, 1 H), 9.16 (s, 1 H), 12.20 (bs, 1 H). MS (APCI$^+$) m/z = 476.3 (M + H$^+$). Anal. (C$_{30}$H$_{29}$N$_5$O·2HCl·2H$_2$O) C, H, N, Cl.

*1-[1-(4-Cyanobenzyl)-1H-imidazol-5-yl]methyl-4-(2-phenylbenzoyl)-1,4-diazepane Hydrochloride (**18**).* 55% yield. R_f = 0.42 (CH$_2$Cl$_2$/MeOH 9:1). Mp: >250 °C. IR (neat): ν 2230 (CN), 1627 (CO). ^{1}H NMR (DMSO-d_6): δ 3.12−3.77 (m, 10 H), 4.45 (s, 2 H), 5.77 (s, 2 H), 7.38−7.60 (m, 11 H), 7.92 (d, J = 7.9 Hz, 2 H), 8.09 (s, 1 H), 9.18 (s, 1 H), 12.09 (bs, 1 H). MS (APCI$^+$) m/z = 476.2 (M + H$^+$). Anal. (C$_{30}$H$_{29}$N$_5$O·2HCl·2H$_2$O) C, H, N, Cl.

*1-[1-(4-Cyanobenzyl)-1H-imidazol-5-yl]methyl-4-cyclohexanoyl-1,4-diazepane Hydrochloride (**19**).* 58% yield. R_f = 0.45 (CH$_2$Cl$_2$/MeOH 9:1). Mp: 212−214 °C. IR (neat): ν 2229 (CN), 1630 (CO). ^{1}H NMR (DMSO-d_6): δ 1.15−1.40 (m, 6 H), 1.55−1.80 (m, 5 H), 2.95−3.15 (m, 2H), 3.30−3.65 (m, 6H), 3.85−4.20 (m, 2 H), 4.44 (s, 2 H), 5.80 (s, 2 H), 7.54 (d, J = 8.3 Hz, 2 H), 7.92 (d, J = 8.1 Hz, 2 H), 8.14 (s, 1H), 9.24 (s, 1 H), 12.10 (bs, 1 H). MS (APCI$^+$) m/z = 406.2 (M + H$^+$). Anal. (C$_{24}$H$_{31}$N$_5$O·2HCl·2H$_2$O) C, H, N, Cl.

*1-[1-(4-Cyanobenzyl)-1H-imidazol-5-yl]methyl-4-(1-adamantanoyl)-1,4-diazepane Hydrochloride (**20**).* 58% yield. R_f = 0.29 (CH$_2$Cl$_2$/MeOH 9:1). Mp: 206−207 °C. IR (neat): ν 2229 (CN), 1631 (CO). ^{1}H NMR (DMSO-d_6): δ 1.68 (s, 6 H), 1.80−2.00 (m, 9 H), 3.00−3.12 (m, 2 H), 3.30−3.60 (m, 6 H), 3.85−4.15 (m, 2 H), 4.46 (s, 2 H), 5.82 (s, 2 H), 7.56 (d, J = 8.4 Hz, 2 H), 7.92 (d, J = 8.1 Hz, 2 H), 8.19 (s, 1 H), 9.29 (s, 1 H), 12.11 (bs, 1 H). MS (APCI$^+$) m/z = 458.3 (M + H$^+$). Anal. (C$_{28}$H$_{35}$N$_5$O·2HCl·2H$_2$O) C, H, N, Cl.

*1-[1-(4-Cyanobenzyl)-1H-imidazol-5-yl]methyl-4-(3-methylbutyroyl)-1,4-diazepane Hydrochloride (**21**).* 63% yield. R_f = 0.65 (CH$_2$Cl$_2$/MeOH 9:1). Mp: 160−161 °C. IR (neat): ν 2228 (CN), 1623 (CO). ^{1}H NMR (DMSO-d_6): δ 0.91 (d, J = 7.1 Hz, 6 H), 2.07−2.21 (m, 1 H), 2.40 (d, J = 6.0 Hz, 2 H), 3.15−3.85 (m, 10 H), 4.51 (s, 2 H), 5.84 (s, 2 H), 7.41−7.57 (m, 2 H), 7.83−7.95 (m, 2 H), 8.18 (bs, 1 H), 9.12 (s, 1 H), 12.13 (bs, 1 H). MS (APCI$^+$) m/z = 380 (M + H$^+$). Anal. (C$_{22}$H$_{29}$N$_5$O·2HCl·1.5H$_2$O) C, H, N, Cl.

7-Phenyl-2,3,4,5-tetrahydro-1H-1,4-diazepin-5-one (22). Ethanediamine (4.7 g, 78 mmol) was added to ethyl benzoylacetate (15 g, 78 mmol) in dry xylene (50 mL). The mixture was heated at 135 °C with an azeotropic Dean−Stark apparatus until the end of water−EtOH distillation. After cooling to room temperature, the reaction mixture was concentrated under vacuum. The residue was washed with diethyl ether, filtered, and dried to give a white powder (8.8 g, 60% yield). R_f (CH$_2$Cl$_2$/MeOH 9:1): 0.25. Mp: 206−207 °C. IR (neat): ν 1626 (CO), 1550 (C=C). ^{1}H NMR (DMSO-d_6): δ 3.49−3.53 (m, 2 H), 3.64−3.68 (m, 2 H), 4.91 (m, 1 H), 5.00 (s, 1 H), 6.10 (m, 1 H), 7.38−7.41 (m, 3 H), 7.51−7.53 (m, 2 H).

7-Phenyl-1,4-diazepan-5-one (23). Palladium (10%) on activated carbon (0.5 g, 0.47 mmol) was added to diazepinone **22** (4.4 g, 2.3 mmol) in MeOH (55 mL), and the mixture was stirred with H$_2$ (50 bar) in an autoclave. After 24 h at 60 °C, the catalyst was filtered off and the filtrate was concentrated under vacuum. The residue was purified by chromatography (CH$_2$Cl$_2$/MeOH 9:1) to give a white powder (4.10 g, 95% yield). R_f = 0.15. Mp: 45 °C. IR (neat): ν 1670 (CO). ^{1}H NMR (CDCl$_3$): δ 2.00 (m, 1 H), 2.59 (d, J = 14.0 Hz, 1 H), 2.95−3.00 (m, 2 H), 3.17−3.22 (m, 2 H), 3.47−3.55 (m, 1 H), 3.91 (d, J = 10.0 Hz, 1 H), 7.25 (m, 1 H), 7.28−7.37 (m, 5 H). MS (APCI$^+$) m/z = 191 (M + H$^+$).

1-tert-Butoxycarbonyl-7-phenyl-1,4-diazepan-5-one (24). Diazepanone **23** (20 g, 88.5 mmol) and DIEA (38 mL, 220 mmol) were dissolved in 300 mL of a mixture of dioxane/water (4:1). Di-*tert*-butyl dicarbonate (22 g, 97 mmol) was added slowly to the solution, stirred for 48 h at room temperature, and concentrated under vacuum. The residue was extracted with EtOAc and then washed with water and brine. The organic layer was dried over MgSO$_4$ and concentrated under vacuum. The residue was purified by chromatography on silica gel (CH$_2$Cl$_2$/MeOH 95:5) to give a white powder (2.45 g, 95% yield). R_f = 0.65. Mp:

134−135 °C. IR (neat): ν 1681 (CO), 1672 (CO). ^{1}H NMR (CDCl$_3$): δ 1.38 (s, 9 H), 2.59 (d, J = 14.0 Hz, 1 H), 2.95−3.00 (m, 2 H), 3.17−3.22 (m, 2 H), 3.47−3.55 (m, 1 H), 3.91 (d, J = 10.0 Hz, 1 H), 7.25−7.30 (m, 1 H), 7.28−7.37 (m, 5 H). MS (ESI) m/z = 290 (M$^+$).

4-tert-Butoxycarbonyl-5-phenyl-1,4-diazepane (25). To a solution of lactam **24** (25 g, 86 mmol) in anhydrous THF (200 mL), LiAlH$_4$ (6.5 g, 172 mmol) was added slowly at 0 °C. After the mixture was stirred for 24 h at room temperature, the reaction was quenched by the dropwise addition of water (50 mL) and sodium hydroxide (7 g, 172 mmol) at 0 °C. The precipitate was filtered off, and the filtrate was concentrated. The residue was purified by chromatography on silica gel (CH$_2$Cl$_2$/MeOH 95:5) to give a yellow oil (1.9 g, 40% yield). R_f = 0.62 (CH$_2$Cl$_2$/MeOH 9/1). IR (neat): ν 1697 (CO). ^{1}H NMR (CDCl$_3$): δ 1.50 (s, 9 H), 1.85−1.89 (m, 1 H), 2.03−2.12 (m, 1H), 2.13 (m, 1H,), 2.82−2.95 (m, 1H), 3.13−3.19 (m, 1H), 3.36−3.75 (m, 5H), 7.21−7.45 (m, 5 H). MS (APCI$^+$) m/z = 277 (M + H$^+$).

4-tert-Butoxycarbonyl-1-{[1-(4-cyanobenzyl)-1H-imidazol-5-yl]methyl}-5-phenyl-1,4-diazepane (26). Amine **25** (1 g, 3.6 mmol), 5-chloromethyl-1-(4-cyanobenzyl)imidazole (1.1 g, 3,6 mmol), and diisopropylethylamine (2.4 mL, 2.4 mmol) were added to 50 mL of acetonitrile and stirred at 80 °C. After 4 h, the solvent was concentrated under vacuum. The residue was diluted with EtOAc and washed by water and brine. The organic layer was dried over MgSO$_4$, filtered, and evaporated. The residue was purified by column chromatography on silica gel (CH$_2$Cl$_2$/MeOH 97:3) to obtain a yellow oil (0.93 g, 55% yield). R_f = 0.65 (CH$_2$Cl$_2$/MeOH 9:1). IR: ν 2229 (CN), 1689 (CO). ^{1}H NMR (CDCl$_3$): δ 1.50 (s, 9 H,), 1.85−1.89 (m, 1 H,), 2.03−2.12 (m, 1 H), 2.82−2.95 (m, 1 H), 3.13−3.19 (m, 1 H), 3.36−3.75 (m, 7 H), 5.47 (s, 2 H), 6.78−6.80 (m, 1H), 7.21−7.58 (m, 10 H).

1-{[1-(4-Cyanobenzyl)-1H-imidazol-5-yl]methyl}-5-phenyl-1,4-diazepane Hydrochloride (27). An amount of 2 mL of a solution of hydrochloric acid (5−6 N) in ^{i}PrOH were added to carbamate **26** (1 g, 2.12 mmol) in 3 mL of MeOH. After the mixture was stirred for 2 h at room temperature, the solvent was concentrated under vacuum. An amount of 100 mL of EtOAc was added to the residue dissolved in minimum EtOH. The precipitate was filtered to obtain a white powder (0.97 g, 95% yield). R_f = 0.05 (CH$_2$Cl$_2$/MeOH 9:1). Mp: > 250 °C. IR (neat): ν 2229 CN). ^{1}H NMR (D$_2$O): δ 1.85−1.89 (m, 1 H), 2.03−2.12 (m, 1 H), 2.82−2.95 (m, 1 H), 3.13−3.19 (m, 1 H), 3.36−3.75 (m, 7 H), 5.45 (s, 2 H), 6.93−6.96 (m, 1 H), 7.19−7.59 (m, 10 H).

General Procedure for the Preparation of 1-{[1-(4-Cyanobenzyl)-1H-imidazol-5-yl]methyl}-5-phenyl-1,4-diazepanes (Compounds 28−33). To 30 mL of a solution of amine **27** in dry N,N-dimethylformamide were added carboxylic acid, EDCI-HCl, pyridine, and DMAP. After the mixture was stirred for 18 h at room temperature, the solvent was concentrated under vacuum. The residue was extracted by EtOAc and washed successively with K$_2$CO$_3$ (10% aq), water, and brine. After drying over MgSO$_4$, the organic layer was evaporated under vacuum. The residue was purified by chromatography on silica gel (CH$_2$Cl$_2$/MeOH 95:5). The product obtained was then added to a solution of 5−6 N HCl in ^{i}PrOH and stirred for 1 h at room temperature. After addition of diethyl ether, the solid was filtered, washed with diethyl ether, and recrystallized by EtOH/Et$_2$O to give a white powder.

*4-Benzoyl-1-{[1-(4-cyanobenzyl)-1H-imidazol-5-yl]methyl}-5-phenyl-1,4-diazepane Hydrochloride (**28**).* 85% yield. R_f = 0.70 (CH$_2$Cl$_2$/MeOH 9:1). Mp: 185−186 °C. IR (neat): ν 2231 (CN), 1652 (CO). ^{1}H NMR (D$_2$O): δ 1.78−2.15 (m, 2 H,), 2.78−2.89 (m, 1 H), 3.07−3.16 (m, 1 H), 3.36−3.75 (m, 7 H), 3.95 (s, 2 H), 5.25 (s, 2 H), 7.01−7.75 (m, 16 H). MS (APCI$^+$) m/z = 476 (M + H$^+$). Anal. (C$_{30}$H$_{29}$N$_5$O·2HCl·1.5H$_2$O) C, H, N, Cl.

*4-(2,4-Dichlorobenzoyl)-1-{[1-(4-cyanobenzyl)-1H-imidazol-5-yl]methyl}-5-phenyl-1,4-diazepane Hydrochloride (**29**).* 82% yield. R_f = 0.70 (CH$_2$Cl$_2$/MeOH 9:1). Mp: 188−189 °C. IR (neat): ν 2229 (CN),

1649 (CO). ^{1}H NMR (DMSO-d_6): δ 1.88−2.21 (m, 2 H), 2.82−2.95 (m, 1 H), 3.08−3.15 (m, 1 H), 3.33−3.81 (m, 5 H), 4.01 (s, 2 H), 5.18 (s, 2 H), 7.01−7.72 (m, 13 H), 8.81 (s, 1 H), 12.11 (bs, 1 H). MS (APCI$^+$) m/z = 510 (M + H$^+$), Anal. (C$_{30}$H$_{27}$Cl$_2$N$_5$O·2HCl·1H$_2$O) C, H, N, Cl.

4-(2-Biphenoyl)-1-{[1-(4-cyanobenzyl)-1H-imidazol-5-yl]methyl}-5-phenyl-1,4-diazepane Hydrochloride (30). 78% yield. R_f = 0.78 (CH$_2$Cl$_2$/MeOH 9:1). Mp: >250 °C. IR (neat): ν 2229 (CN), 1649 (CO). ^{1}H NMR (D$_2$O): δ 1.81−1.87 (m, 1 H), 2.07−2.16 (m, 1 H), 2.84−3.73 (m, 7 H), 3.97 (s, 2 H), 5.44 (s, 2 H), 6.92−6.99 (m, 1 H), 7.06−7.70 (m, 19 H). MS (APCI$^+$) m/z = 552 (M + H$^+$). Anal. (C$_{36}$H$_{33}$N$_5$O·2HCl·1.5H$_2$O) C, H, N, Cl.

1-{[1-(4-Cyanobenzyl)-1H-imidazol-5-yl]methyl}-4-(1-naphthoyl)-5-phenyl-1,4-diazepane Hydrochloride (31). 75% yield. R_f = 0.75 (CH$_2$Cl$_2$/MeOH 9:1). Mp: 205 °C. IR (neat): ν 2227 (CN), 1649 (CO). ^{1}H NMR (DMSO-d_6): δ 1.85−1.89 (m, 1 H), 2.03−2.12 (m, 1 H), 2.87−3.13−3.21 (m, 2 H), 3.36−3.75 (m, 7 H), 5.41 (s, 2 H) ; 6.93−6.96 (m, 1 H), 7.15−8.15 (m, 16 H), 8.84 (s, 1 H), 12.01 (bs, 1 H). MS (APCI$^+$) m/z = 526 (M + H$^+$). Anal. (C$_{34}$H$_{31}$N$_5$O·2HCl· 1.5H$_2$O) C, H, N, Cl.

1-{[1-(4-Cyanobenzyl)-1H-imidazol-5-yl]methyl}-4-cyclohexanoyl-5-phenyl-1,4-diazepane Hydrochloride (32). 68% yield. R_f = 0.62 (CH$_2$Cl$_2$/MeOH 9: 1). Mp: 125 °C. IR (neat): ν 2229 (CN), 1649 (CO). ^{1}H NMR (D$_2$O): δ 1.15−1.40 (m, 6 H), 1.55−1.80 (m, 5 H), 1.85−1.89 (m, 1 H), 2,03−2,12 (m, 1 H), 2.82−2.95 (m, 1 H), 3.13−3.19 (m, 1 H), 3.36−3.75 (m, 7 H), 5.45 (s, 2 H), 6.93−6.96 (m, 1 H), 7.17−7.63 (m, 10 H). MS (APCI$^+$) m/z = 482 (M + H$^+$). Anal. (C$_{30}$H$_{35}$N$_5$O·2HCl·1,5H$_2$O) C, H, N, Cl.

4-(1-Adamantanoyl)-1-{[1-(4-cyanobenzyl)-1H-imidazol-5-yl]methyl}-5-phenyl-1,4-diazepane Hydrochloride (33). 67% yield. R_f = 0.64 (CH$_2$Cl$_2$/MeOH 9:1). Mp: >250 °C. IR (neat): ν 2229 (CN), 1649 (CO). ^{1}H NMR (D$_2$O): δ 1.68 (s, 6 H), 1.80−2.00 (m, 9 H), 1.85−1.89 (m, 1 H), 2.03−2.12 (m, 1 H), 2.82−2.95 (m, 1 H), 3.13− 3.19 (m, 1 H), 3.36−3.75 (m, 7 H), 5.45 (s, 2 H), 6.93−6.96 (m, 1 H), 7.21−7.65 (m, 10 H). MS (APCI$^+$) m/z = 534 (M + H$^+$). Anal. (C$_{34}$H$_{39}$N$_5$O·2HCl·1.5H$_2$O) C, H, N, Cl.

General Procedure for the Preparation of 4-*tert*-Butoxy-carbonyl-5-phenyl-1,4-diazepanes (Compounds 34−39). Amine **25** was used for the acylation step. The procedure was adapted from the synthesis of compounds **28−33**.

1-Benzoyl-4-tert-butoxycarbonyl-5-phenyl-1,4-diazepane (34). 77% yield. R_f = 0.87 (CH$_2$Cl$_2$/MeOH 9:1). IR (neat): ν 1682 (CO), 1649 (CO). ^{1}H NMR (DMSO-d_6): δ 1.33 (s, 9 H), 1.55−1.61 (m, 1 H), 2.13−2.21 (m, 1 H), 2.71−3.77 (m, 6 H), 3.82−3.99 (m, 1 H), 7.11−7.55 (m, 8 H), 7.72−7.91 (m, 2 H).

1-(2,4-Dichlorobenzoyl)-4-tert-butoxycarbonyl-5-phenyl-1,4-diazepane (35). 95% yield. R_f = 0.95 (CH$_2$Cl$_2$/MeOH 9:1). IR (neat): ν 1691 (CO), 1649 (CO). ^{1}H NMR (DMSO-d_6): δ 1.38 (s, 9 H), 1.85−1.89 (m, 1 H), 2.03−2.12 (m, 1 H), 2.82−2,95 (m, 1 H), 3.13−3.19 (m, 1 H), 3.36−3.75 (m, 5 H), 7.11−7.55 (m, 8 H).

1-(2-Biphenoyl)-4-tert-butoxycarbonyl-5-phenyl-1,4-diazepane (36). 95% yield. R_f = 0.95 (CH$_2$Cl$_2$/MeOH 9:1). IR (neat): ν 1680 (CO), 1649 (CO). ^{1}H NMR (DMSO-d_6): δ 1.50 (s, 9 H), 1.85−1.89 (m, 1 H), 2.03−2.12 (m, 1 H), 2.82−2.95 (m, 1 H), 3.13−3.19 (m, 1 H), 3.34−3.72 (m, 5 H), 7.11−7.80 (m, 14 H).

1-(1-Naphthoyl)-4-tert-butoxycarbonyl-5-phenyl-1,4-diazepane (37). 95% yield. R_f = 0.95 (CH$_2$Cl$_2$/MeOH 9:1). IR (neat): ν 1685 (CO), 1649 (CO). ^{1}H NMR (DMSO-d_6): δ 1.50 (s, 9 H,), 1.85−1.89 (m, 1 H), 1.98−2.02 (m, 1 H), 2.84−2.97 (m, 1 H), 3.15−3.20 (m, 1 H), 3.36−3.75 (m, 5 H), 7.11−7.65 (m, 12 H).

1-Cyclohexanoyl-4-tert-butoxycarbonyl-5-phenyl-1,4-diazepane (38). 70% yield. R_f = 0.85 (CH$_2$Cl$_2$/MeOH 9:1). IR (neat): ν 1686 (CO), 1649 (CO). ^{1}H NMR (DMSO-d_6): δ 1.10−1.38 (m, 6 H), 1.39 (s, 9 H), 1.45−1.78 (m, 5 H), 1.81−1.92 (m, 1 H), 2.08−2.21 (m, 1 H),

2.82−2.95 (m, 1 H), 3.13−3.19 (m, 1 H), 3.38−3.73 (m, 5 H), 7.09−7.38 (m, 5 H).

1-(1-Adamantanoyl)-4-tert-butoxycarbonyl-5-phenyl-1,4-diazepane (39). 88% yield. R_f = 0,85 (CH$_2$Cl$_2$/MeOH 9:1). IR (neat): ν 1690 (CO), 1649 (CO). ^{1}H NMR (DMSO-d_6): δ 1.55−1.72 (m, 15 H), 1.75−1.95 (m, 9 H), 1.98−2.05 (m, 1 H), 2.03−2.12 (m, 1 H), 2.81−2.93 (m, 1 H), 3.10−3.17 (m, 1 H), 3.36−3.75 (m, 5 H), 7.11−7.45 (m, 5 H).

General Method for the Preparation of 5-Phenyl-1,4-diazepanes (Compounds 40−45). Corresponding Boc derivatives (**34−39**) were used for the synthesis of target compounds **40−45**. The procedure was the same as for the synthesis of compound **2**.

1-Benzoyl-5-phenyl-1,4-diazepane Hydrochloride (40). 95% yield. R_f = 0.15 (CH$_2$Cl$_2$/MeOH 9:1). Mp: 175 °C. IR (neat): ν 1653 (C═O amide). ^{1}H NMR (DMSO-d_6): δ 1.88−1.98 (m, 1 H), 2.09−2.21 (m, 1 H), 2.76−2.97 (m, 1 H), 3.13−3.19 (m, 1 H), 3.36−3.75 (m, 5 H), 7.11−7.55 (m, 10 H), 8.53 (bs, 2 H).

1-(2,4-Dichlorobenzoyl)-5-phenyl-1,4-diazepane Hydrochloride (41). 95% yield. R_f = 0.20 (CH$_2$Cl$_2$/MeOH 9:1). Mp: 205 °C. IR (neat): ν 1649 (CO). ^{1}H NMR (DMSO-d_6): δ 1.7−1.94 (m, 1 H), 2.01−2.10 (m, 1 H), 2.80−2.91 (m, 1 H), 3.11−3.15 (m, 1 H), 3.38−3.77 (m, 5 H), 7.11−7.55 (m, 8 H), 8,48 (bs, 2 H).

1-(2-Biphenoyl)-5-phenyl-1,4-diazepane Hydrochloride (42). 95% yield. R_f = 0.20 (CH$_2$Cl$_2$/MeOH 9:1). Mp: 188 °C. IR (neat): ν 1649 (CO). ^{1}H NMR (DMSO-d_6): δ 1.79−1.86 (m, 1 H), 2.05−2.16 (m, 1 H), 2.86−2.97 (m, 1 H), 3.14−3.21 (m, 1 H), 3.33−3.71 (m, 5 H), 7.11−7.65 (m, 14 H), 8,61 (bs, 2 H).

1-(1-Naphthoyl)-5-phenyl-1,4-diazepane Hydrochloride (43). 95% yield. R_f = 0.20 (CH$_2$Cl$_2$/MeOH 9:1). Mp: 188 °C. IR (neat): ν 1649 (CO). ^{1}H NMR (DMSO-d_6): δ 1.87−1.91 (m, 1 H), 2.05−2.14 (m, 1 H), 2.84−2.96 (m, 1 H), 3.16−3.22 (m, 1 H), 3.41−3.81 (m, 5 H), 7.17−7.62 (m, 11 H), 8.83 (s, 1 H).

1-Cyclohexanoyl-5-phenyl-1,4-diazepane Hydrochloride (44). 95% yield. R_f = 0.10 (CH$_2$Cl$_2$/MeOH 9:1). Mp: 195 °C. IR (neat): ν 1649 (CO). ^{1}H NMR (DMSO-d_6): δ 1.15−1.40 (m, 6 H), 1.55−1.80 (m, 5 H), 1.85−1.89 (m, 1 H), 2.03−2.12 (m, 1 H), 2.82−2.95 (m, 1 H), 3.13−3.19 (m, 1 H), 3.36−3.75 (m, 5 H), 7.11−7.45 (m, 5 H), 8,32 (bs, 2H).

1-(1-Adamantanoyl)-5-phenyl-1,4-diazepane Hydrochloride (45). 95% yield. R_f = 0.10 (CH$_2$Cl$_2$/MeOH 9:1). Mp: 188 °C. IR (neat): ν 1649 (CO). ^{1}H NMR (DMSO-d_6): δ 1.68 (s, 6 H), 1.82−2.05 (m, 9 H), 1.98−2.05 (m, 1 H), 2.08−2.17 (m, 1 H), 2.91−3.03 (m, 1 H), 3.17−3.29 (m, 1 H), 3.14−3.66 (m, 5 H), 7.17−7.49 (m, 5 H), 8,36 (bs, 2 H).

General Procedure for the Preparation of 4-{[1-(4-Cyanobenzyl)-1H-imidazol-5-yl]methyl}-5-phenyl-1,4-diazepanes (Compounds 46−51). Corresponding diazepanes **40−45** were used for the preparation of target compounds (**46−51**). The procedure was adapted from the methodology used for the synthesis of compound **1**. The residues were purified by chromatography on silica gel (CH$_2$Cl$_2$/MeOH 95:5).

1-Benzoyl-4-{[1-(4-cyanobenzyl)-1H-imidazol-5-yl]methyl}-5-phenyl-1,4-diazepane Hydrochloride (46). 55% yield. R_f = 0.69 (CH$_2$Cl$_2$/MeOH 9:1). Mp: 185 °C. IR (neat): ν 2229 (CN), 1649 (CO). ^{1}H NMR (D$_2$O): δ 1.45−1.57 (m, 1 H), 1.73−1.85 (m, 1 H$_2$), 2.55−2.68 (m, 1 H), 3.01−3.12 (m, 1 H), 3.22−3.61 (m, 7 H), 5.11 (s, 2 H), 6.93−6.96 (m, 1 H), 7.13−7.62 (m, 15 H). MS (APCI$^+$) m/z = 476 (M + H$^+$). Anal. (C$_{30}$H$_{29}$N$_5$O·2HCl·1.5H$_2$O) C, H, N, Cl.

1-(2,4-Dichlorobenzoyl)-4-{[1-(4-cyanobenzyl)-1H-imidazol-5-yl]methyl}-5-phenyl-1,4-diazepane Hydrochloride (47). 95% yield. R_f = 0.70 (CH$_2$Cl$_2$/MeOH 9:1). Mp: 188 °C. IR (neat): ν 2229 (CN), 1649 (CO). ^{1}H NMR (D$_2$O): δ 1.91−1.99 (m, 1 H), 2.01−2.09 (m, 1 H), 2.76−2.91 (m, 1 H), 3.13−3.19 (m, 1 H), 3.36−3.75 (m, 7 H), 5.30 (s, 2 H), 7.05−7.63 (m, 14 H). MS (APCI$^+$) m/z = 510 (M + H$^+$). Anal. (C$_{30}$H$_{27}$N$_5$OCl$_2$·2HCl·1H$_2$O), C, H, N, Cl.

*1-(2-Biphenoyl)-4-{[1-(4-cyanobenzyl)-1H-imidazol-5-yl]methyl}-5-phenyl-1,4-diazepane Hydrochloride (**48**).* 62% yield. R_f = 0.70 (CH$_2$Cl$_2$/MeOH 9:1). Mp: >250 °C. IR (neat): ν 2229 (CN), 1649 (CO). ^{1}H NMR (D$_2$O): δ 1.70−2.03 (m, 2 H), 2.55−3.55 (m, 5 H), 4.17−4.26 (m, 1 H), 4.48 (s, 2 H), 5.45 (s, 2 H), 7.05−7.70 (m, 19 H). MS (APCI$^+$) m/z = 552 (M + H$^+$). Anal. (C$_{36}$H$_{35}$N$_5$O·2HCl·1.5H$_2$O), C, H, N, Cl

*1-(1-Naphthoyl)-4-{[1-(4-cyanobenzyl)-1H-imidazol-5-yl]methyl}-5-phenyl-1,4-diazepane Hydrochloride (**49**).* 51% yield, R_f = 0.81 (CH$_2$Cl$_2$/MeOH 9:1). Mp: 208 °C. IR (neat): ν 2227 (CN), 1654 (CO). ^{1}H NMR (DMSO-d_6): δ 1.78−1.86 (m, 1 H), 1.91−2.06 (m, 1 H), 2.75−2.82 (m, 1 H), 3.01−3.11 (m, 1 H), 3.36−3.75 (m, 5 H), 4.12 (s, 2 H), 5.05 (s, 2 H), 6.93−6.96 (m, 1 H), 7.05−8.17 (m, 17 H), 8.84 (s, 1 H), 10.32 (bs, 2 H). MS (APCI$^+$) m/z = 526 (M + H$^+$). Anal. (C$_{34}$H$_{31}$N$_5$O·2HCl·1.5H$_2$O), C, H, N, Cl.

*1-Cyclohexanoyl-4-{[1-(4-cyanobenzyl)-1H-imidazol-5-yl]methyl}-5-phenyl-1,4-diazepane Hydrochloride (**50**).* 82% yield. R_f = 0.70 (CH$_2$Cl$_2$/MeOH 9:1). Mp: 125 °C. IR (neat): ν 2229 (CN), 1649 (CO). ^{1}H NMR (D$_2$O): δ 1.17−1.41 (m, 6 H), 1.63−1.96 (m, 6 H), 2.02−2.10 (m, 1 H), 3.12−3.75 (m, 7 H), 4.17 (s, 2 H), 5.15 (s, 2 H), 6.95−6.99 (m, 1 H), 7.18−7.65 (m, 10 H). MS (APCI$^+$) m/z = 482 (M + H$^+$). Anal. (C$_{30}$H$_{35}$N$_5$O·2HCl·1.5H$_2$O) C, H, N, Cl.

*1-(1-Adamantanoyl)-4-{[1-(4-cyanobenzyl)-1H-imidazol-5-yl]methyl}-5-phenyl-1,4-diazepane Hydrochloride (**51**).* 57% yield. R_f = 0.59 (CH$_2$Cl$_2$/MeOH 9:1). Mp: >250 °C. IR (neat): ν 2229 (CN), 1649 (CO). ^{1}H NMR (D$_2$O): δ 1.59 (s, 6 H), 1.78−2.08 (m, 10 H), 3.36−3.75 (m, 7 H), 4.10−4.18 (m, 1 H), 4.28 (s, 2 H), 5.30 (s, 2 H), 6.93−6.96 (m 1 H), 7.21−7.45 (m, 10 H). MS (APCI$^+$) m/z = 534 (M + H$^+$). Anal. (C$_{34}$H$_{39}$N$_5$O·2HCl·1.5H$_2$O) C, H, N, Cl.

Molecular Modeling. Molecular modeling studies were performed using SYBYL[39] software, version 6.92, running on a Silicon Graphics workstation. Three-dimensional models of selected compounds were built from a standard fragments library, and their geometry was subsequently optimized using the Tripos force field including the electrostatic term calculated from Gasteiger and Hückel atomic charges. Powell's method, available in the Maximin2 procedure, was used for energy minimization until the gradient value was smaller than 0.001 kcal/(mol·Å). The structure of the human FTase was obtained from its complexed X-ray crystal structure of the RCSB Protein Data Bank (1LD7) with FPP and the inhibitor molecule described by Bell.[40] Flexible docking of FTis into the enzyme's active site was performed using GOLD software.[39] The distance observed in the crystal structure between the distal nitrogen imidazole and the zinc cation was applied as a constraint. For each compound, the most stable docking model was selected according to the best conformation predicted by the GoldScore and X-Score scoring functions.[41] The complexes were energy-minimized using the Powell method available in the Maximin2 procedure with the Tripos force field and a dielectric constant of 4.0 until the gradient value reached 0.01 kcal/(mol·Å).

FTase Fluorescent Assay Procedure. Assays were realized on 96-well plates, prepared with Biomek NKMC and Biomek 3000 from Beckman Coulter and read on a Wallac Victor fluorimeter from Perkin-Elmer. To each well, 20 μL of farnesyl pyrophosphate (10 μM) was added to 180 μL of a solution containing 2 μL of varied concentrations of potent inhibitor (dissolved in DMSO) and 178 μL of a solution composed of 100 μL of partially purified recombinant yeast FTase (2.2 mg/mL) and 7.0 mL of dansyl-GCVLS peptide (2 μM) in the following buffer: 5.5 mM DTT, 10 mM MgCl$_2$, 10 μM ZnCl$_2$ and 0.08% (w/v) CHAPS, and 50 mM Tris/HCl, pH 7.5. Then the fluorescence development was recorded for 15 min (0.7 s per well, 20 repeats) at 30 °C with an excitation filter at 340 nm and an emission filter at 486 nm.

Cell Culture. The human prostate cancer lines PC3 and DU145 were obtained from ATCC. Cells were grown in RPMI 1640 (Gibco, Invitrogen Corp.) supplemented with 10% fetal bovine serum (Gibco, Invitrogen Corp.), 2 mM glutamine, and 5 units/mL of streptomycin and 5 units/mL of penicillin. All cells were cultured at 37 °C in a humidified incubator with 5% CO$_2$.

MTT Cytotoxicity Assay. Cytotoxicity of selected drugs was tested using the MTT (thiazolyl blue tetrazolium bromide) assay based on the cellular uptake of MTT (Sigma Aldrich) and its subsequent reduction in the mitochondria of living cells to dark blue MTT formazan crystals (Mosmann, 1983). Cells were seeded on 96-well plates ((1.6−1.8) × 10^4 cells/well) in the corresponding medium supplemented with 10% FBS. Seventy-two hours later, cells were deprived of FBS. The next day, they were treated with various concentrations of each tested compound. Following the 72 h exposure to the cytotoxic drugs, cell survival was determined by incubation with MTT (4 mg/mL) for 4 h (37 °C, 5% CO$_2$). The cells were then lyzed in SDS/HCl and plates left in the incubator to dissolve the purple formazan crystals. The color intensity reflecting cell viability was read with a spectrophotometer Elx 800 (Biotek Instruments Inc.) at 570 nm.

siRNA transfection. siRNA transfection was realized with CENP-E siRNA 10616 (Ambion) and transfection reagent DharmaFECT2 (Dharmacon RNA Technologies) according to the manufacturer's instructions. Cells were incubated at 37 °C for 48 h.

Immunofluorescence. Cells were plated on poly-D-lysine coated coverslips (BD-Biocoat) and incubated overnight at 37 °C and 5% CO$_2$. After synchronization, cells were treated with FTIs for 24 h. The cells were fixed in 4% paraformaldehyde and then permeabilized with 0.5% Triton X-100/PBS. After blocking for 45 min in 5% BSA/PBS, cells were washed with PBS and incubated with anti-α-tubulin antibody conjugated with Alexa 488 (dilution 1/100) and with anti-CENP-E antibody (dilution 1/100) followed by addition of a secondary antibody conjugated with Alexa 568 (dilution 1/400). The samples were then washed and mounted in Mowiol. Cells were visualized using a fluorescence microscope (Nikon, Eclipse 80i).

■ ASSOCIATED CONTENT

Ⓢ Supporting Information. Results from elemental analysis. This material is available free of charge via the Internet at http://pubs.acs.org.

■ AUTHOR INFORMATION

Corresponding Author
*Phone: +33-3-2096-4374. Fax: +33-3-2096-4906. E-mail: régis.millet@univ-lille2.fr.

■ ACKNOWLEDGMENT

■ ABBREVIATIONS USED

ACN, acetonitrile; CA-4, combretastatin A-4; CENP-E, centromere protein E; CENP-F, centromere protein F; CLogP, calculated log P; DCM, dichloromethane; DIEA, N,N-diisopropylethylamine; DMAP, 4-(N,N-dimethylamino)pyridine; DMF, N,N-dimethylformamide; DMSO, dimethylsulfoxide; EDCI, 1-ethyl-3-(3-dimethylaminopropyl)carbodiimide; EtOAc, ethyl acetate; EtOH, ethanol; FPP, farnesylpyrophosphate; FTase, protein farnesyltransferase; FTis, farnesyltransferase inhibitors; GADPH, glyceraldehyde 3-phosphate dehydrogenase; GGPP, geranylgeranyl

pyrophosphate; GGTase-I, protein geranylgeranyltransferase I; HOBt, 1-hydroxybenzotriazole; HPLC, high performance liquid chromatography; IC$_{50}$, half-maximal inhibitory concentration; ^{i}PrOH, isopropanol; PBS, phosphate buffered saline; PyBroP, bromotrispyrrolidinophosphonium hexafluorophosphate; rt, room temperature; SAR, structure—activity relationship; TLC, thin layer chromatography

■ REFERENCES

(1) Reid, T. S.; Terry, K. L.; Casey, P. J.; Beese, L. S. Crystallographic analysis of CaaX prenyltransferases complexed with substrates defines rules of protein substrate selectivity. *J. Mol. Biol.* **2004**, *343*, 417–433.

(2) Casey, P. J.; Seabra, M. C. Protein prenyltransferases. *J. Biol. Chem.* **1996**, *271*, 5289–5292.

(3) Bell, I. M. Inhibitors of farnesyltransferase: a rational approach to cancer chemotherapy?. *J. Med. Chem.* **2004**, *47*, 1869–1878.

(4) Sepp-Lorenzino, L.; Ma, Z.; Rands, E.; Kohl, N. E.; Gibbs, J. B.; Oliff, A.; Rosen, N. A peptidomimetic inhibitor of farnesyl:protein transferase blocks the anchorage-dependent and -independent growth of human tumor cell lines. *Cancer Res.* **1995**, *55*, 5302–5309.

(5) Taylor, S. A.; Marrinan, C. H.; Liu, G.; Nale, L.; Bishop, W. R.; Kirschmeier, P.; Liu, M.; Long, B. J. Combining the farnesyltransferase inhibitor lonafarnib with paclitaxel results in enhanced growth inhibitory effects on human ovarian cancer models in vitro and in vivo. *Gynecol. Oncol.* **2008**, *109*, 97–106.

(6) Moasser, M. M.; Sepp-Lorenzino, L.; Kohl, N. E.; Oliff, A.; Balog, A.; Su, D. S.; Danishefsky, S. J.; Rosen, N. Farnesyl transferase inhibitors cause enhanced mitotic sensitivity to taxol and epothilones. *Proc. Natl. Acad. Sci. U.S.A.* **1998**, *95*, 951369–951374.

(7) Shi, B.; Yaremko, B.; Hajian, G.; Terracina, G.; Bishop, W. R.; Liu, M.; Nielsen, L. L. The farnesyl protein transferase inhibitor SCH66336 synergizes with taxanes in vitro and enhances their antitumor activity in vivo. *Cancer Chemother. Pharmacol.* **2000**, *46*, 387–393.

(8) Nakamura, K.; Yamaguchi, A.; Namiki, M.; Ishihara, H.; Nagasu, T.; Kowalczyk, J. J.; Garcia, A. M.; Lewis, M. D.; Yoshimatsu, K. Antitumor activity of ER-51785, a new peptidomimetic inhibitor of farnesyl transferase: synergistic effect in combination with paclitaxel. *Oncol. Res.* **2001**, *12*, 477–484.

(9) Zhu, K.; Gerbino, E.; Beaupre, D. M.; Mackley, P. A.; Muro-Cacho, C.; Beam, C.; Hamilton, A. D.; Lichtenheld, M. G.; Ker, W. G.; Dalton, W.; Alsina, M.; Sebti, S. M. Farnesyltransferase inhibitor R115777 (Zarnestra, tipifarnib) synergizes with paclitaxel to induce apoptosis and mitotic arrest and to inhibit tumor growth of multiple myeloma cells. *Blood* **2005**, *105*, 4759–4766.

(10) Schafer-Hales, K.; Iaconelli, J.; Snyder, J. P.; Prussia, A.; Nettles, J. H.; El-Naggar, A.; Khuri, F. R.; Giannakakou, P.; Marcus, A. I. Farnesyl transferase inhibitors impair chromosomal maintenance in cell lines and human tumors by compromising CENP-E and CENP-F function. *Mol. Cancer Ther.* **2007**, *6*, 1317–1328.

(11) Grönberg, H. Prostate cancer epidemiology. *Lancet* **2003**, *361*, 859–864.

(12) Long, S. B.; Hancock, P. J.; Kral, A. M.; Hellinga, H. W.; Beese, L. S. The crystal structure of human protein farnesyltransferase reveals the basis for inhibition by CaaX and their mimetics. *Proc. Natl. Acad. Sci. U.S.A.* **2001**, *96*, 12948–12953.

(13) Long, S. B.; Casey, P. J.; Beese, L. S. Reaction path of protein farnesyltransferase at atomic resolution. *Nature* **2002**, *419*, 645–650.

(14) Reid, T. S.; Long, S. B.; Beese, L. S. Crystallographic analysis reveals that anticancer clinical candidate L-778,123 inhibits protein farnesyltransferase and geranylgeranyltransferase-I by different binding modes. *Biochemistry* **2004**, *43*, 9000–9008.

(15) Reid, T. S.; Besse, L. S. Crystal structure of the anticancer clinical candidates R115777 (tipifarnib) and BMS-214662 complexed with protein farnesyltransferase suggest a mechanism of FTis selectivity. *Biochemistry* **2004**, *43*, 6877–6884.

(16) Houssin, R.; Pommery, J.; Salaün, M. C.; Deweer, S.; Goossens, J. F.; Chavatte, P.; Hénichart, J. P. Design, synthesis, and pharmacological evaluation of new farnesyl protein transferase inhibitors. *J. Med. Chem.* **2002**, *17* (45), 533–536.

(17) Millet, R.; Domarkas, J.; Houssin, R.; Gilleron, P.; Goossens, J. F.; Chavatte, P.; Logé, C.; Pommery, N.; Pommery, J.; Hénichart, J. P. Potent and selective farnesyl transferase inhibitors. *J. Med. Chem.* **2004**, *47*, 6812–6820.

(18) Gilleron, P.; Millet, R.; Houssin, R.; Wlodarczyk, N.; Farce, A.; Lemoine, A.; Goossens, J. F.; Chavatte, P.; Pommery, N.; Hénichart, J. P. Solid-phase synthesis and pharmacological evaluation of a library of peptidomimetics as potential farnesyltransferase inhibitors: an approach to new lead compounds. *Eur. J. Med. Chem.* **2006**, *41*, 745–755.

(19) Wlodarczyk, N.; Gilleron, P.; Millet, R.; Houssin, R.; Goossens, J. F.; Lemoine, A.; Pommery, N.; Wei, M. X.; Hénichart, J. P. In vitro and in vivo evaluation of two rational-designed nonpeptidic farnesyltransferase inhibitors on HT29 human colon cancer cell lines. *Oncol. Res.* **2005**, *16*, 107–118.

(20) Maligres, P. E.; Waters, M. S.; Weissman, S. A.; McWilliams, J. C.; Lewis, S.; Cowen, J.; Reamer, R. A.; Volante, R. P.; Reider, P. J.; Askin, D. Preparation of a clinically investigated Ras farnesyl transferase inhibitor. *J. Heterocycl. Chem.* **2003**, *40*, 229–241.

(21) Pop, I. E.; Deprez, B. P.; Tartar, A. L. Versatile acylation of N-nucleophiles using a new polymer-supported 1-hydroxybenzotriazole derivative. *J. Org. Chem.* **1997**, *62*, 2594–2603.

(22) Stern, E.; Muccioli, G. G.; Millet, R.; Goossens, J. F.; Farce, A.; Chavatte, P.; Poupaert, J. H.; Lambert, D. M.; Depreux, P.; Hénichart, J. P. Novel 4-oxo-1,4-dihydroquinoline-3-carboxamide derivatives as new CB2 cannabinoid receptors agonists: synthesis, pharmacological properties and molecular modelling. *J. Med. Chem.* **2006**, *49*, 70–79.

(23) Wlodarczyk, N.; Gilleron, P.; Millet, R.; Houssin, R.; Hénichart, J. P. Synthesis of 1,4-diazepin-5-ones under microwave irradiation and their reduction products. *Tetrahedron Lett.* **2007**, *48*, 2583–2586.

(24) Dolence, J. M; Cassidy, P. B; Mathis, J. R; Poulter, C. D. Yeast protein farnesyltransferase: steady-state kinetic studies of substrate binding. *Biochemistry* **1995**, *34*, 16687–16694.

(25) Sepp-Lorenzino, L.; Ma, Z.; Rands, E.; Kohl, N. E.; Gibbs, J. B.; Oliff, A.; Rosen, N. A peptidomimetic inhibitor of farnesyl:protein transferase blocks the anchorage-dependent and -independent growth of human tumor cell lines. *Cancer Res.* **1995**, *55*, 5302–5309.

(26) Sepp-Lorenzino, L.; Tjaden, G.; Moasser, M. M.; Timaul, N.; Ma, Z.; Kohl, N. E.; Gibbs, J. B.; Oliff, A.; Rosen, N.; Scher, H. I. Farnesylprotein transferase inhibitors as potential agents for the management of human prostate cancer. *Prostate Cancer Prostatic Dis.* **2001**, *4*, 33–43.

(27) Sirotnak, F. M.; Sepp-Lorenzino, L.; Kohl, N. E.; Rosen, N.; Scher, H. I. A peptidomimetic inhibitor of ras functionality markedly suppresses growth of human prostate tumor xenografts in mice. Prospects for long-term clinical utility. *Cancer Chemother. Pharmacol.* **2000**, *46*, 79–83.

(28) CLogP values were calculated using software ACD/LogP developed by www.acdlabs.com.

(29) Bell, I. M.; Gallichio, S. N.; Abrams, M.; Beshore, D. C.; Buser, C. A.; Culberson, J. C.; Davide, J.; Ellis-Hutchings, M.; Christine Fernandes, C.; Gibbs, J. B.; Graham, S. L.; Hartman, G. D.; Heimbrook, D. C.; Homnick, C. F.; Huff, J. R.; Kassahun, K.; Koblan, K. S.; Kohl, N. E.; Lobell, R. B.; Lynch, J. J., Jr.; Miller, P. A.; Omer, C. A.; Rodrigues, A. D.; Walsh, E. S.; Williams, T. M. Design and biological activity of (S)-4-(5-{[1-(3-chlorobenzyl)-2-oxopyrrolidin-3-ylamino]methyl}imidazol-1-ylmethyl)benzonitrile, a 3-aminopyrrolidinone farnesyltransferase inhibitor with excellent cell potency. *J. Med. Chem.* **2001**, *44*, 2933–2949.

(30) Wang, L.; Wang, G. T.; Wang, X.; Tong, Y.; Sullivan, G.; Park, D.; Leonard, N. M.; Li, Q.; Cohen, J.; Gu, W. Z.; Zhang, H.; Bauch, J. L.; Jakob, C. G.; Hutchins, C. W.; Stoll, V. S.; Marsh, K.; Rosenberg, S. H.; Sham, H. L.; Lin, N. H. Design, synthesis, and biological activity of 4-[(4-cyano-2-arylbenzyloxy)-(3-methyl-3H-imidazol-4-yl)methyl]benzonitriles as potent and selective farnesyltransferase inhibitors. *J. Med. Chem.* **2004**, *47*, 612–626.

(31) Studies were performed at Cerep according to their internal procedures.

(32) Guidance for Industry. Waiver of in Vivo Bioavailability and Bioequivalence Studies for Immediate-Release Solid Oral Dosage Forms Based on a Biopharmaceutics Classification System. FDA: Rockville, MD, 2000.

(33) Jones, G.; Willett, P.; Glen, R. C.; Leach, A. R.; Taylor, R. Development and validation of a genetic algorithm for flexible docking. *J. Mol. Biol.* **1997**, *267*, 727–748.

(34) Bell, I. M.; Gallichio, S. N.; Abrams, M.; Beese, L. S.; Beshore, D. C.; Bhimnathwala, H.; Bogusky, M. J.; Buser, C. A.; Culberson, J. C.; Davide, J.; Ellis-Hutchings, M.; Fernandes, C.; Gibbs, J. B.; Graham, S. L.; Hamilton, K. A.; Hartman, G. D.; Heimbrook, D. C.; Homnick, C. F.; Huber, H. E.; Huff, J. R.; Kassahun, K.; Koblan, K. S.; Kohl, N. E.; Lobell, R. B.; Lynch, J. J., Jr.; Robinson, R.; Rodrigues, A. D.; Taylor, J. S.; Walsh, E. S.; Williams, T. M.; Zartman, C. B. 3-Aminopyrrolidinone farnesyltransferase inhibitors: design of macrocyclic compounds with improved pharmacokinetics and excellent cell potency. *J. Med. Chem.* **2002**, *45*, 2388–2409.

(35) Pettit, G. R.; Singh, S. B.; Hamel, E.; Lin, C. M.; Alberts, D. S.; Garcia-Kendall, D. Isolation and structure of the strong cell growth and tubulin inhibitor combretastatin A-4. *Experientia* **1989**, *45*, 209–211.

(36) Lin, C. M.; Ho, H. H.; Pettit, G. R.; Hamel, E. Antimitotic natural products combretastatin A-4 and combretastatin A-2: studies on the mechanism of their inhibition of the binding of colchicine to tubulin. *Biochemistry* **1989**, *28*, 6984–6991.

(37) Hussein, D.; Taylor, S. S. Farnesylation of CENP-F is required for G2/M progression and degradation after mitosis. *J. Cell Sci.* **2002**, *115*, 3403–3414.

(38) Marcus, A. I; Zhou, J.; O'Brate, A.; Hamel, E.; Wong, J.; Nivens, M.; El-Naggar, A.; Yao, T.-P.; Khuri, F. R.; Giannakakou, P. The synergistic combination of the farnesyl transferase inhibitor lonafarnib and paclitaxel enhances tubulin acetylation and requires a functional tubulin deacetylase. *Cancer Res.* **2005**, *65*, 3883–3893.

(39) *SYBYL*, version 6.92; Tripos Associates, Inc. (1699 South Hanley Road, St. Louis, MO 63144).

(40) Bell, I. M.; Gallichio, S. N.; Abrams, M.; Beese, L. S.; Beshore, D. C.; Bhimnathwala, H.; Bogusky, M. J.; Buser, C. A.; Culberson, J. C.; Davide, J.; Ellis-Hutchings, M.; Fernandes, C.; Gibbs, J. B.; Graham, S. L.; Hamilton, K. A.; Hartman, G. D.; Heimbrook, D. C.; Homnick, C. F.; Huber, H. E.; Huff, J. R.; Kassahun, K.; Koblan, K. S.; Kohl, N. E.; Lobell, R. B.; Lynch, J. J., Jr.; Robinson, R.; Rodrigues, A. D.; Taylor, J. S.; Walsh, E. S.; Williams, T. M.; Zartman, C. B. 3-Aminopyrrolidinone farnesyltransferase inhibitors: design of macrocyclic compounds with improved pharmacokinetics and excellent cell potency. *J. Med. Chem.* **2002**, *45*, 2388–2409.

(41) Wang, R.; Lai, L.; Wang, S. Further development and validation of empirical scoring functions for structure-based binding affinity prediction. *J. Comput.-Aided Mol. Des.* **2002**, *16*, 11–26.